Response to Referee #1

We appreciate all comments from the reviewer, which help to further improve the quality of our manuscript. In this round of revision, we have considered all comments seriously. The point-by-point revisions have been made and tracked in the change-noted manuscript. We hope that the new version of manuscript has met the requirements from the referee and ANGEO. In the following, the comments are marked in bold Times New Roman, followed by our responses.

This is an interesting paper for investigating the currents at low and middle latitudes during intense geomagenetic storms. The results showed that there exist also southward/northward currents in the inner plasma sheet, but they are neither the ring currents nor field aligned currents. The authors suggest that such horizontal currents at low and middle latitudes are caused by the curvature drift of energetic particles during magnetic storms.

In general, the paper is well written, and the observational results support their conclusion. However, before it is accepted by Annales Geophysicae, some comments listed below may need to be taken into account.

Major comments:

1. **The authors focus only the northern middle latitudes in their study. One interesting question would be to check the southern low and middle latitudes, to see if similar currents can also be observed. If yes, it might indicate that such currents are field-aligned. If not, the authors could provide some explanation or suggestions.**

Response:

Thank you for your good suggestion. Actually, the southward and northward current also can be observed in the southern low and middle latitudes. The following two figures show the geometry of the magnetic field and the current distribution in the southern hemisphere for the two events concerned in this work. We can see similar fluctuations with what we observed in the manuscript.

So, the reported southward and northward current can observed both in north and south hemisphere. However, they are not the field-aligned currents. Actually, we have also given field-aligned current component (j_B) in last panel of the figure. The observed southward and northward current is the component perpendicular to j_B.

Anyway, it is a good suggestion to mention result from south hemisphere. We have added a short discussion in 'Discussion' part, see lines 14-16 in page 16 of the change-noted manuscript.

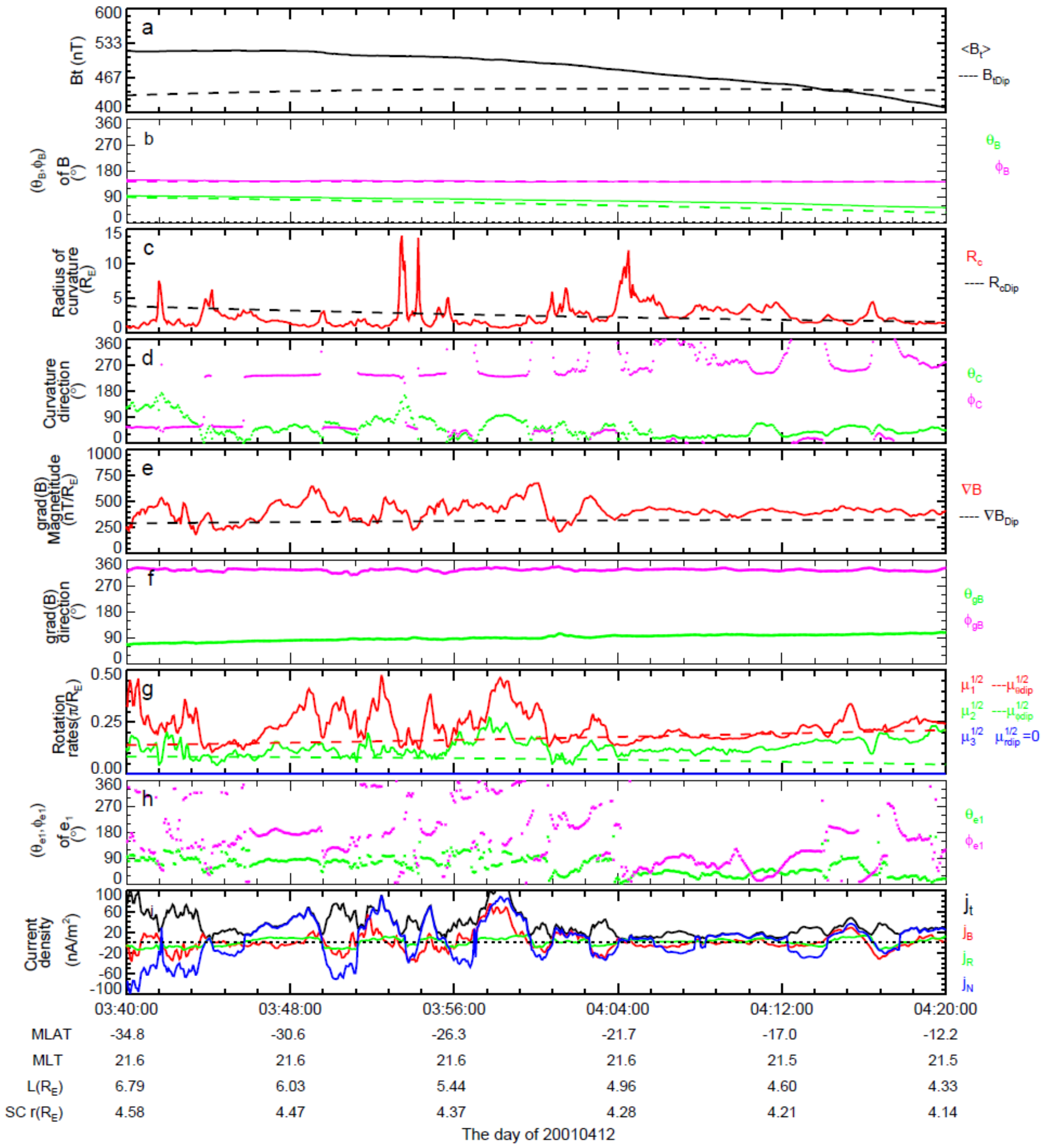

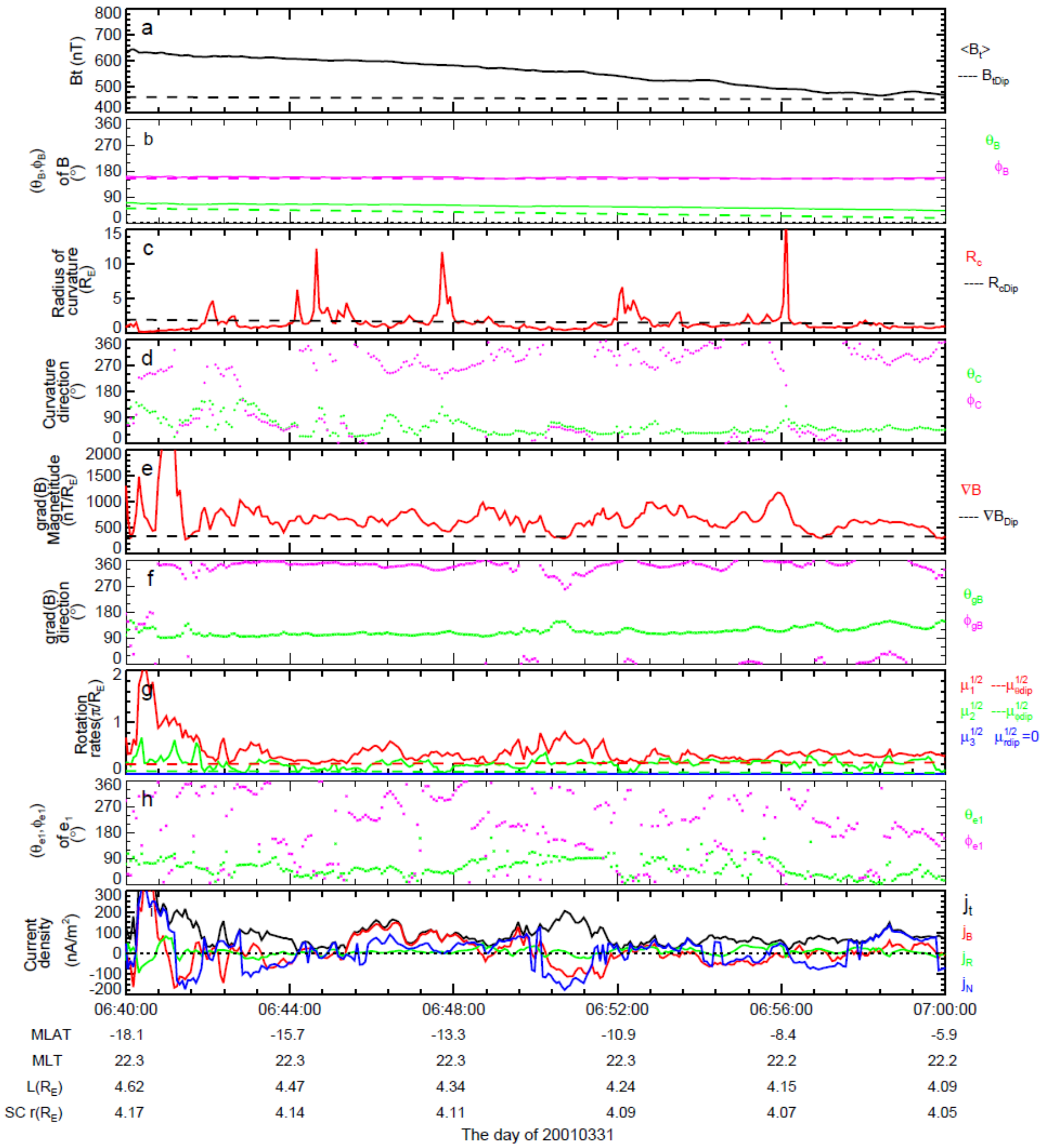

2. It seems there is no real summary in the end of the study. The author may think to add a typical summary.

Response:

Thank you for your suggestion, we have added the summary section in the manuscript, see lines 5-18 in page 18 and lines 1-3 in page 19 of the change-noted manuscript.

Some minor comments

Abstract:

1. during large storm events -> during intense geomagnetic storms

Response:

Changed. See line 12 in page 1 of the change-noted manuscript.

2. which cannot be FACs -> which should not be FACs

Response:

Modified. See line 13 in page 1 of the change-noted manuscript.

3. highly fluctuate -> high dynamic

Response:

Revised. See line 15 in page 1 of the change-noted manuscript.

Introduction

4. Page 1, line 20: "Recently, through simulations and observations, numerous studies have shown that the inner magnetosphere currents have a more complicated structure and distribution than originally thought".

The author are suggested to provide more detailed description of "more complicated structure and distribution than originally though", not just added references there.

Response:

Thank you, we have provided more detailed description in the new version of manuscript. See lines 22-27 in page 1 of the change-noted manuscript.

5. Page 1, line 26: respectively, from high latitude and low latitude -> from high and low latitudes, respectively.

Response:

Modified. See lines 2-3 in page 2 of the change-noted manuscript.

6. Page 2, line 6: in the latitude regions from 10 °N to 50 °N

In the abstract, the authors claimed that they focus on the latitude range between 10-30 °N.

Response:

Thanks to point out our mistake, it should be from 10-30° **N**. We have made a modification. See line 11 in page 2 of the change-noted manuscript.

3. Event analysis

7. Page 7, line 7: (The event was once reported by Shen et al. (2014), but they only concentrated on the interval from ~07:00 to 7:25 UT). ->

The event was once reported by Shen et al. (2014), but they only concentrated on the interval from ~07:00 to 7:25 UT.

Response:

Changed. See lines 7-8 in page 8 of the change-noted manuscript.

8. Page 7, lines 11-12:

It can be seen that these parameters behave as same as that of the first event, but with stronger magnetic field strength.

Response:

Modified. See lines 11-12 in page 8 of the change-noted manuscript.

9. page 7, line 14:

And the largest rotation rate (Figure 3g) oscillates significantly and exhibits…

Response:

Revised. See lines 14-15 in page 8 of the change-noted manuscript.

4. Summary and Discussion

It should be Discussion and Summary

Response:

Since we have added a summary in the last part, we modified this part as 'Discussion'. See line 4 in page 10 of the change-noted manuscript.

10. Page 10, line 12:

ε and α are the particle energy and pitch angle, respectively.

Response:

Modified. See line 12-13 in page 12 of the change-noted manuscript.

11. Page 11, line 11:

During the strong storm time, turbulences, e.g., the ULF waves, result in the fluctuation of the MFLs, …

Response:

Modified. See line 11 in page 13 of the change-noted manuscript.

12.Provide a typical summary of this work at the end of the study.

Response:

Provided. See lines 5-18 in page 18 and lines 1-3 in page 19 of the change-noted manuscript.

Response to Referee #2

We appreciate all comments from the reviewer, which help to enhance our understanding of current in this region and improve the quality of our manuscript. In this round of review, we have considered all comments seriously. The point-by-point revisions have been made and tracked in the change-noted manuscript. We hope that our revised manuscript can meet the requirement from referee and ANGEO. In the following, the comments are marked in bold Times New Roman, followed by our responses.

The authors present an original research manuscript which aims to explain observations performed in the northern nightside magnetosphere, where northward and southward currents are detected along with oscillations in the field curvature. In this region, the dominant currents are field-aligned currents and the ring current, which should exist mostly in the X-Y-plane. The authors propose that these currents are due to curvature drifts of energetic particles. The authors base their analysis on two mid-latitude storm time vents and Cluster spacecraft data, and various analysis techniques using multiple instruments from the Cluster mission.

The manuscript has generally good structure, a well-chosen selection of figures and good language. The authors take into account some of the important potential sources of errors in their analysis. The topic of research is interesting, and indeed worth pursuing. However, I have some fundamental questions regarding the logic behind this analysis and the application of the methods, and would appreciate if the authors could substantially clarify the issue, as well as improve the methods which would make the results more robust.

Major issue: The authors present MRA-method analysis of magnetic curvature and compare it with measured current densities, postulating that the current is due to curvature drift. However, the whole method of measuring currents aboard

Cluster is based on the Curlometer technique, which calculates the curl (curvature) of a magnetic field and calculates the current from that. I feel that the authors need to give more reasoning as to why they consider it a new finding that one magnetic curvature analysis technique explains currents calculated via another magnetic curvature analysis technique.

Response:

As stated in the 'Methodology' part, MRA has the ability to calculate current density, so, we use MRA method, rather than Curlometer method to directly deduce the current density in this work. So, from this point of view, we didn't use one magnetic curvature analysis technique explains currents calculated via another magnetic curvature analysis technique.

Secondly, the calculation of current density using MRA method is also based on Maxwell-Ampere's law:

$$\mathbf{J} = \frac{1}{\mu_0} \nabla \times \mathbf{B} \qquad (1)$$

From this formula, we can obtain three components of current density. However, the current density calculated from this formula includes all contributions and we cannot obtain any behind mechanism information. For example, in the inner magnetosphere, we cannot distinguish the current contribution from gradient drifts, curvature drift and the gyromotion only from this formula.

Though, Eq (1) cannot reflect any information about contributions from each part, the following three formulas can.

$$\mathbf{j}_{\nabla} = P_{\perp} \frac{\mathbf{B} \times \nabla B}{B^3},$$

$$\mathbf{j}_C = -\frac{P_{\parallel}}{B^2} \boldsymbol{\rho}_c \times \mathbf{B}, \qquad (2)$$

$$\mathbf{j}_G = \frac{\mathbf{B}}{B^2} \times \left[\nabla P_{\perp} - \frac{P_{\perp}}{B} \nabla B - \frac{P_{\perp}}{B^2} (\mathbf{B} \cdot \nabla) \mathbf{B} \right],$$

So, when we combine Eq (1) and (2), it becomes possible to distinguish current density from three processes.

Major issue: page 6 lines 13-17: If I'm interpreting this correctly, the coordinate system in use (j_B, j_N, j_R) changes constantly with the magnetic field measurements (as referred to as a local natural coordinate system in the caption of Figure 2). Is this calculated pre- or post IGRF (or dipole field?) deduction? I'm worried that the coordinate system is not well defined when the direction of the curvature changes abruptly. Looking at the evolution of the theta and phi angles for the direction of curvature, it looks to me like j_N is mostly in the east-west-direction, and has a north-south component only at the extrema of the curvature oscillation. A re-decomposition of currents into cartesian or SM coordinates would have been important to answer questions arising from this coordinate selection, and would help with evaluation of results.

A question that arises directly from this, is how much of the observed j_N is actually new current density in the north-south direction, and how much of it is existing ring current simply re-mapped due to an abruptly changing coordinate system?

Response:

Thank you very much for pointing out the use of coordinate system. Yes, the coordinate system in use (j_B, j_N, j_R) changes constantly with the magnetic field measurements. And it is calculated pre-IGRF (it will be pre-dipole field in the new version of manuscript, see the following response) deduction, which intends to reflect the real background magnetic field.

To make things more clearly, we will utilize the local cylindrical coordinate system (j_ρ, j_φ, j_z) in the new version of the manuscript, which is defined first in the work of Vallat et al. 2005 (see following Figure). j_z is parallel to the Z_{SM} axis; j_ρ represents the radial component of the current on the plane parallel to the (X_{SM}, Y_{SM}) plane, oriented anti-earthward; j_φ points eastward.

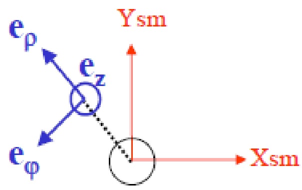

In the following Figure, we replot the three components of the current density in the new coordinate system. To reflect field aligned currents, j_B is also plotted in the figure. From j_z component of the figure, it is very clear to see that the current is along southward and northward direction. Another advantage to use this coordinate system is that we can keep the consistency with Figure 5 and 6 in the manuscript (since we use z direction there).

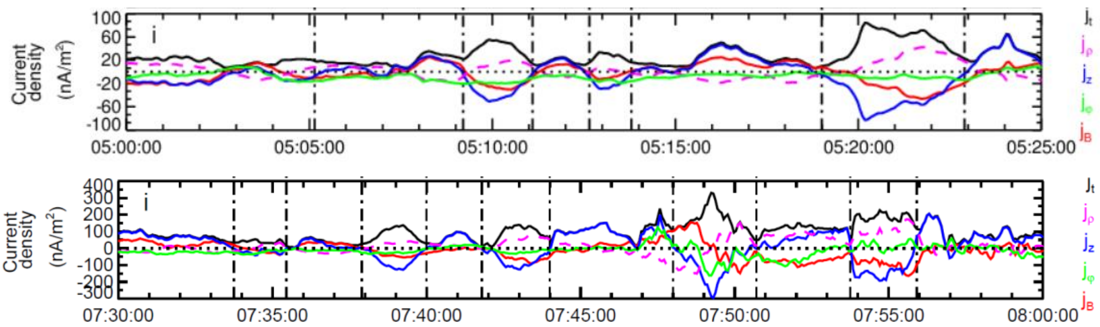

The coordinate system and the corresponding description and plots have been updated in the new version of manuscript. See lines 21-23 in page 2, section 3.1 and 3.2 of the change-noted manuscript.

Major issue: page 12, description of how the authors evaluate plasma pressure via the kappa distribution and CIS/CODIF: I believe the authors should further clarify how they perform this analysis in order to quell concerns regarding the trustworthiness of the method. I shall try to elaborate. A Kappa distribution behaves wholly differently (quasi-Maxwellian) at low energies where CODIF data is available, than at higher energies, in the tail. As seen in Figure 1, the energy spectrogram varies wildly during the storm, and thus, assuming the plasma to be in something like a steady state and describable with a kappa distribution is a bold suggestion. After all, during storms is when there is strong acceleration of particles and deviation from the mean distribution.

The authors could explain in better detail how is the fit performed exactly, and what are the deduced kappa values? Both parameters "a" and "kappa" are being fitted using the low-energy portion of the population - some estimation of the quality and reliability of this fit should be presented.

Response:

Thank you. This is a critical and very interesting comment. Actually, regarding Kappa distribution, we did more works.

(1) Indeed, particles are accelerated during the storm. However, we suppose that Kappa distribution (taking the form $\mathbf{a}\boldsymbol{E}^{-\kappa}$) is still satisfied. But it should be noted that **a** and κ are no longer a constant but varied during the storm. To verify our hypothesis, we make a test using differential flux of H^+ (from CIS/CODIF) for 12 Aril 2001 event. As one example, the following Figure shows the distribution function (with pitch angle is 90°) for 9 different time points during the concerned interval. It can be seen that distribution function has good scaling, which can verify our hypothesis about Kappa distribution.

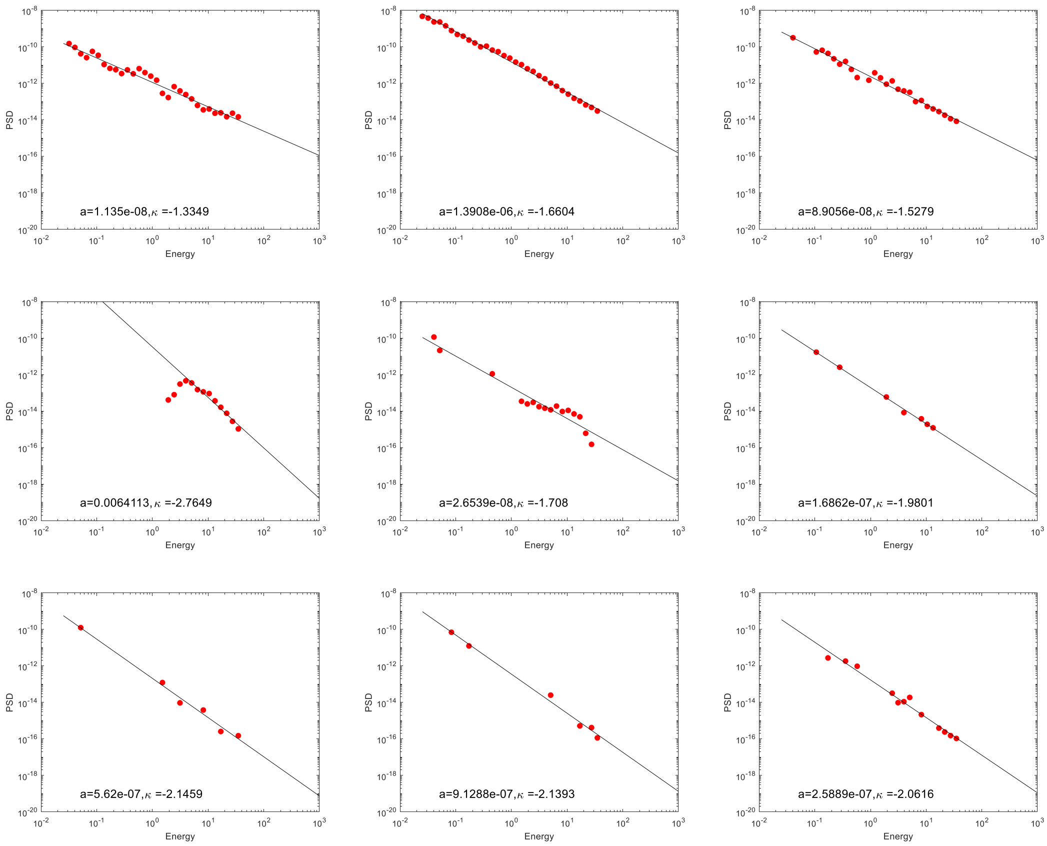

The following Figure displays the corresponding variation of **a** and κ during the whole interval (using Kappa distribution). We can see that both of them are varied.

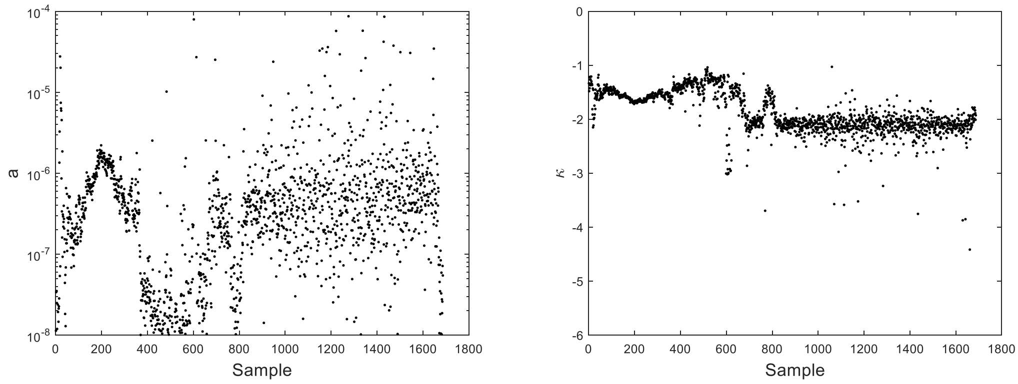

(2) To test if the estimated high energetic particle differential flux (using low energy particle data) is reasonable, the best way is to check with the measurement. For Cluster, RAPID can provide energy spectrograms for high energetic particles. Unfortunately, there is no RAPID data for the two concerned events. Therefore, we have tried to find another storm event to test. The selected event occurred on 20 April 2002, with the minimum of the Dst index is -149nT (we can't find a storm event with similar Dst index in the similar position). The result is presented in the following Figure. The blue dots are observations from low energetic particles (CIS/CODIF) and the red dots are measurement from high energetic particles (RAPID). The black line is the fitted result from low energetic particles. It should be noted that the observations from RAPID is limited. But still, we can see that the fitted result can basically reflect the main trend of the high energetic particles.

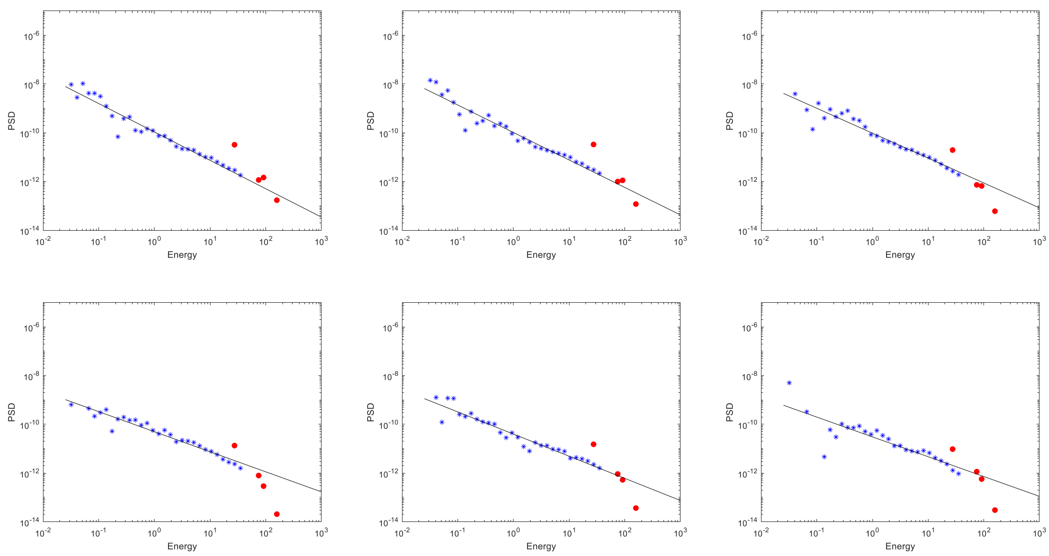

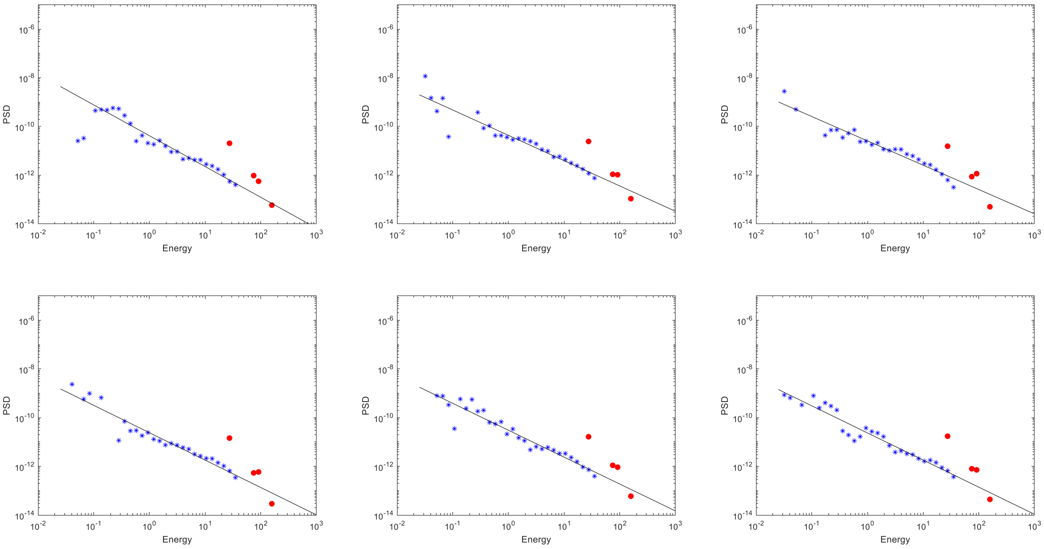

The above analysis demonstrates that our hypothesis about Kappa distribution is reasonable. We believe that the particle distribution during strong storm events is very complicated but interesting topic, and more detailed works are still needed, which is our next research plan. In this work, we mainly concentrate on the mechanism of the current generation. Considering the main target of this work, we think that it is better to give another detailed study and discussion for results mentioned above in the future, rather than put all figures in this manuscript. But we will add more explanation (for the above result) in the manuscript to support our calculation, see line 1 to 7 in page 16 of the change-noted manuscript.

Also, is the population assumed to be isotropic? Equation (3) takes only the parallel pressure, after all. Figure 6 shows the final result, but comparing that with Figure 5 suggests that the pressure contribution to the calculated current is minimal, and rather, it is dominated by the curvature component (as shown in Figure 5). And if the result is dominated by curvature, then of course it will match up with the MRA method (and the inherent curlometer technique). Thus, I am not convinced that energetic particle curvature drifts are particularly important here.

Response:

That's very interesting question. Figure 5 in the manuscript is only used to indicate the direction variation of curvature drift current, it cannot see if curvature component dominates for the current calculation.

Actually, we have verified that the pressure contribution, rather than curvature component (as mentioned by the referee), is the dominate part for the curvature current deduction. Remember lines 11-15 in page 11 to line 1 in page 12 of the manuscript, we have mentioned that when we use low energy particle data from CIS/CODIF, the estimated curvature drift current is less than 1 nA/m^2. If the result dominates by curvature, it is impossible to obtain such small value. However, when we add high energy particle simulation data, the estimated current is close to current density calculated from MRA (see Figure 6 in the manuscript). It implies that the pressure is the main contribution. The role of the curvature component shown in Figure 5 in the manuscript is to keep the curvature drift current direction consistent with what we observed in Figure 2i and 3i (southward or northward current component).

Minor issues / clarification requests:

page 2 line 9: Although others have called the curlometer technique "direct" measurement of the current, in truth, direct calculation would be counting charged particle fluxes. Perhaps briefly state that it uses magnetic curvature to calculate currents via Maxwell-Ampère's law.

Response:

Thank you, as we have mentioned above, we use MRA method to calculate current density, but it also based on Maxwell-Ampère's law. We have modified the sentence. See line 15-16 in page 2 of the change-noted manuscript.

page 2 line 20: A normal can be defined for a plane, not directly for a field line, unless you assume it to be in a plane within which the local curvature is. Please clarify.

Response:

We make a mistake here. It should be 'binormal'. We have corrected the word. See line 2 in page 3 of the change-noted manuscript.

page 2 lines 24-26: Could the authors please clarify, why they state that they subtract the IGRF field, yet then proceed to describe the standard dipole formulation?

Response:

We subtract the IGRF field because it is closer to the real magnetic field. Then, we compare with dipole field in Figure 2 and 3 because we can obtain the radius of curvature, the magnetic field gradient and rotation rates directly from Eq (1) in the manuscript. Actually, we also have tried subtracted the dipole field, the following Figure shows the calculated current density. It can be seen that the main features are the same with what we obtain from IGRF subtraction. We also have checked that the difference of the two calculated current density is less than 1nA/m^2, so, it will not affect the conclusion of this work. To keep the consistency, we will utilize dipole field and updated the figures in the new version of manuscript. See modifications in line 7-8 in page 3 of the change-noted manuscript. Figure 2 and 3 has been updated using calculation from dipole field accordingly.

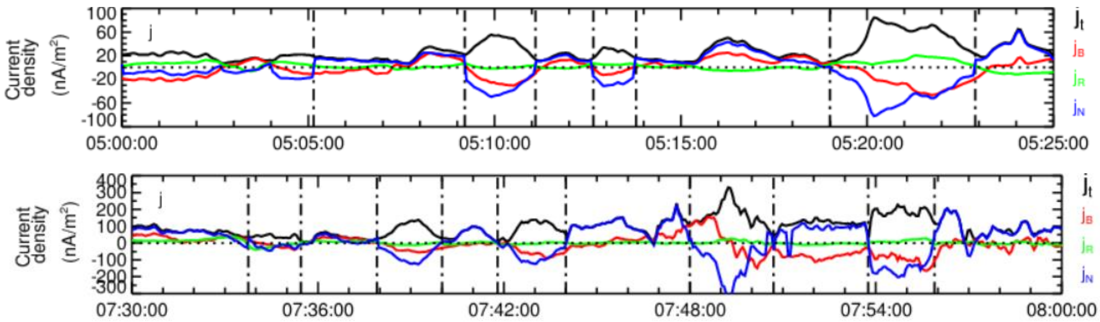

page 5, Figure 2: Could the authors please explain why they plot a dipole field for comparison, instead of the IGRF field they state they use in the text?

Response:

The reason has been explained in last response. We have unified to use only dipole field in the new version of manuscript.

page 6 line 5: Evaluation of Figure 2 panel c shows that contrary to what is written here, the radius of curvature is nearly everywhere much greater than that of the dipole field. Only in NH3 and NH6-8 does it drop below the dipole field value, and only then in the middle of the domain.

Response:

Thank you. The decreased radius of curvature is more visible in second case. It is more reasonable to say that the radius of curvature is varied compare with that of dipole. We have re-write the sentence in the new version of manuscript. See line 8 in page 7 of the change-noted manuscript.

page 8 line 7: Stating that the field lines were severely deviated would be more readily confirmed had the authors included x,y,z components of the magnetic field. The radius of curvature is a challenging method of showing this, as it becomes most important at very small values, which are not clearly visible in the plots.

Response:

From Figure 2a and Figure 3a of the manuscript, it is very easy to recognize that the magnetic field lines are severely deviated from the dipole field.

Besides, we also compared the three components of magnetic field with that of the dipole field (see following Figure). They are indeed deviated from dipole field, which is consistent with the above analysis. We didn't put the figure in the manuscript since they are too many plots.

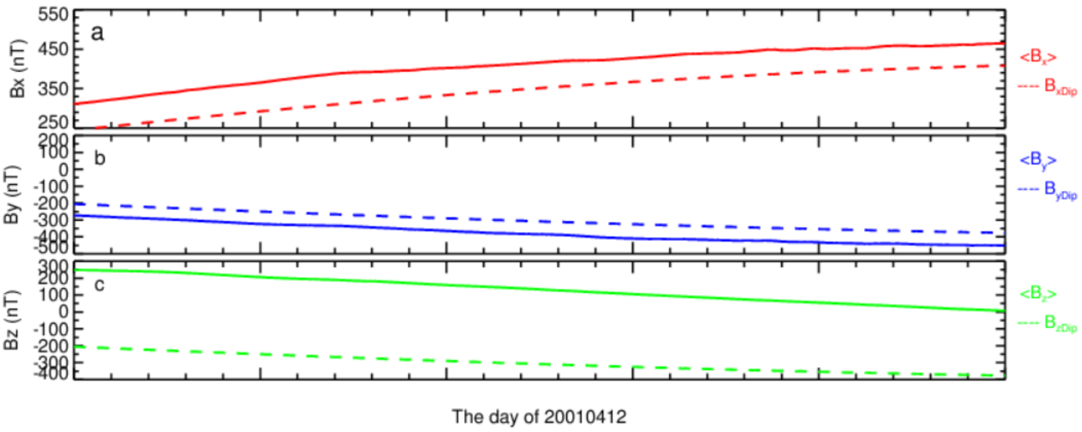

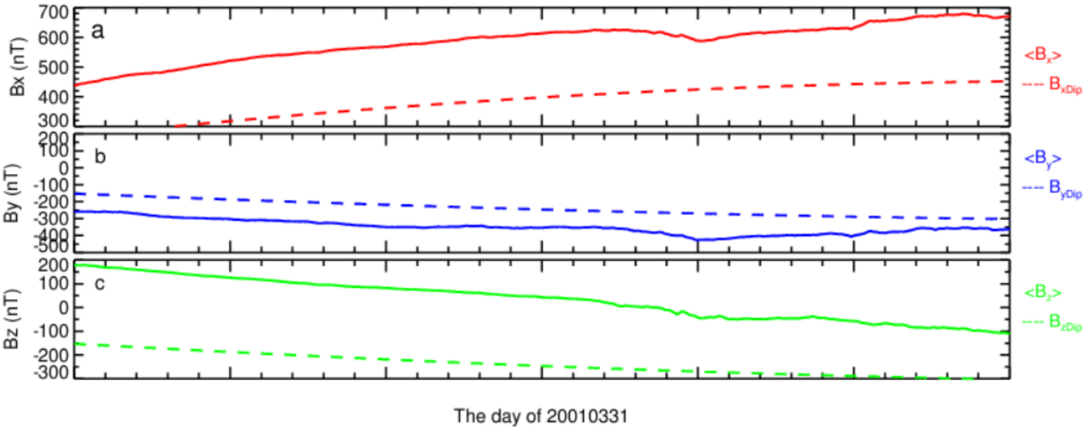

As for radius of curvature, actually, it is a very useful method to properly show the change (stretch) of the field line. To illustrate this feature intuitively, we provide a cartoon plot in the following Figure (note that the change of real field line is exaggerated to better show the variation), for the region we concerned, the radius of curvature of the dipole field points approximately to the Earth. However, the observations of curvature direction (Figure 2d and 3d) show that the real field point to XY plane, i.e., changed (stretched) in XY plane. But, it should keep in mind that this doesn't mean that radius curvature must smaller than that of dipole field. It is completely possible larger than curvature radius of dipole field (for example, the first event).

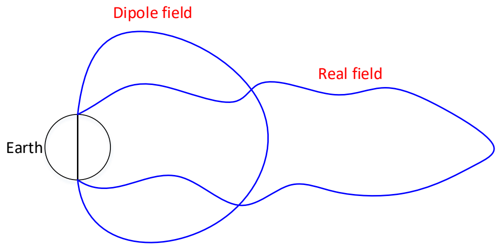

page 10 lines 16-18: The text should reference Figure 5, panels a and b. I would recommend stating more clearly what is being shown and analyzed, instead of simply referring to "a result", which here is simply the cross product of the curvature and the magnetic field. Also, the authors claim that the z component of this has the same variation trend as j_z, but j_z has not been shown in any figure. If the authors claim that this is the same as j_N, the questions regarding stability of the chosen coordinate system apply again. I think the manuscript would be

much improved if these doubts could be clarified.

Response:

As has been illustrated in the above response, to keep consistency, we have utilized the new coordinate system (j_ρ, j_φ, j_z) to describe the current density this time. Now, the j_z component has the same meaning in Figure 2, Figure 3, Figure 5 and Figure 6 of the manuscript.

page 10 line 19-21: I believe the authors should clarify their reasoning for disregarding the possibility of the third term of gyromotion drift to cause currents in the j_z direction.

Response:

According to $\mathbf{j}_G = \frac{\mathbf{B}}{B^2} \times \left[\nabla P_\perp - \frac{P_\perp}{B} \nabla B - \frac{P_\perp}{B^2} (\mathbf{B} \cdot \nabla)\mathbf{B} \right]$, the gyromotion current is originated from three terms, i.e., $\mathbf{B} \times \nabla P_\perp$, - $\mathbf{B} \times \nabla B$ and - $\mathbf{B} \times (\mathbf{B} \cdot \nabla)\mathbf{B}$. Firstly, according to previous works (e.g., Lui et al., 1987; De Michelis et al., 1999), $\nabla P_\perp$ is along the radial direction (see left plot of the following Figure). For two events concerned in this work (Cluster orbit is shown in the right plot of the following Figure), $\nabla P_\perp$ should be in the X-Y plane and along the direction indicated by the red arrow. From Figure 2b and 3b in the manuscript, it is shown that the magnetic field also points to the same direction. It means that $\nabla P_\perp$ has the similar direction with magnetic field. So, the contribution from $\mathbf{B} \times \nabla P_\perp$ should be very small. Secondly, − $\mathbf{B} \times \nabla B$ is similar to the gradient drift current and can be negligible. Thirdly, since $(\mathbf{B} \cdot \nabla)\mathbf{B}$ has the same direction with $\boldsymbol{\rho}_c$ ($\boldsymbol{\rho}_c = (\hat{\mathbf{b}} \cdot \nabla)\hat{\mathbf{b}}, \hat{\mathbf{b}} = \mathbf{B} / |\mathbf{B}|$), according to Figure 5a and 5b, the product of -$\mathbf{B} \times (\mathbf{B} \cdot \nabla)\mathbf{B}$ (similar to $\boldsymbol{\rho}_c \times \mathbf{B}$) will behave oppositely to j_z. Consequently, the gyromotion current has little possibility of contributing to a strong j_z. We have added the above explanation in line 16 of page 12 to line 9 in page

13 of the change-noted manuscript.

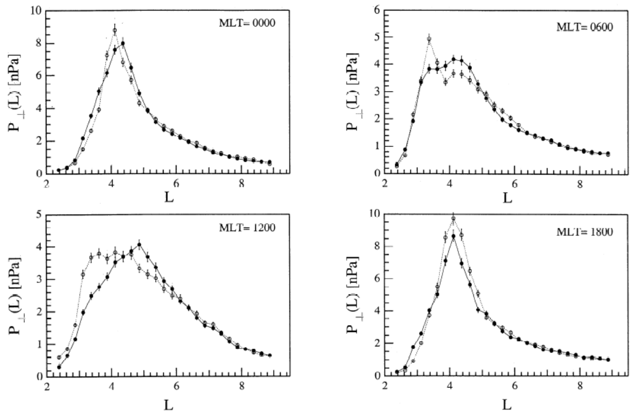

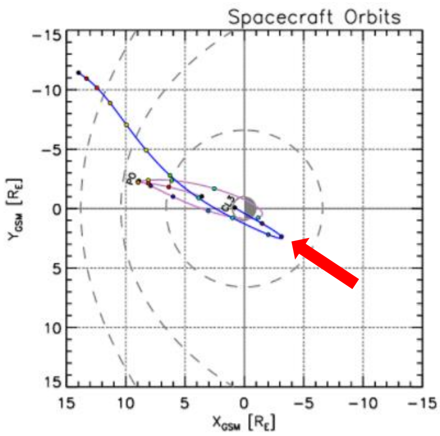

On line 15, they stated that both the magnetic field and its gradient are pointed towards the dayside, so this term might be non-negligible.

Response:

Since the magnetic field $\mathbf{B}$ and its gradient ∇B towards the same direction, the cross product of them ($\mathbf{B}\times\nabla B$) should approximate to zero and can be neglected.

Figure 5: The caption states that the plot shows "results deduced from the radius of curvature of the cross magnetic field" - I would recommend the authors be more explicit and exact in their statements.

Response:

We have re-write the captions in Figure 5. See line 3-5 in page 14 of the change-noted manuscript.

page 13, line 6: Now the authors compare with the T96 model, but provide no reference. Does comparison with the T96 model provide some benefit over using the IGRF or dipole models, which are used(?) in the rest of the analysis? Remaining consistent would improve the readability of the manuscript.

Response:

Thank you. We have added references for T96 model. Since the Tsyganenko model is closer to real magnetic field in the magnetosphere, it is usually used to trace footprints of satellites (see the following Figure, which is obtained from http://ergsc.isee.nagoya-u.ac.jp/cef/orbit.cgi?jump=Submit&year=2019&dateformat=md&month=01&day=01&doy=022&period=0000&interval=1d&plottypeg=midlat&plottypem=ims&size=100). In this work, we didn't make any comparison with T96 model, but just follow the convention and use it to trace the Cluster footprints in the northern hemisphere. To avoid misunderstanding, we have reorganized the sentence in the manuscript. See line 18-20 in page 16 of the change-noted manuscript.

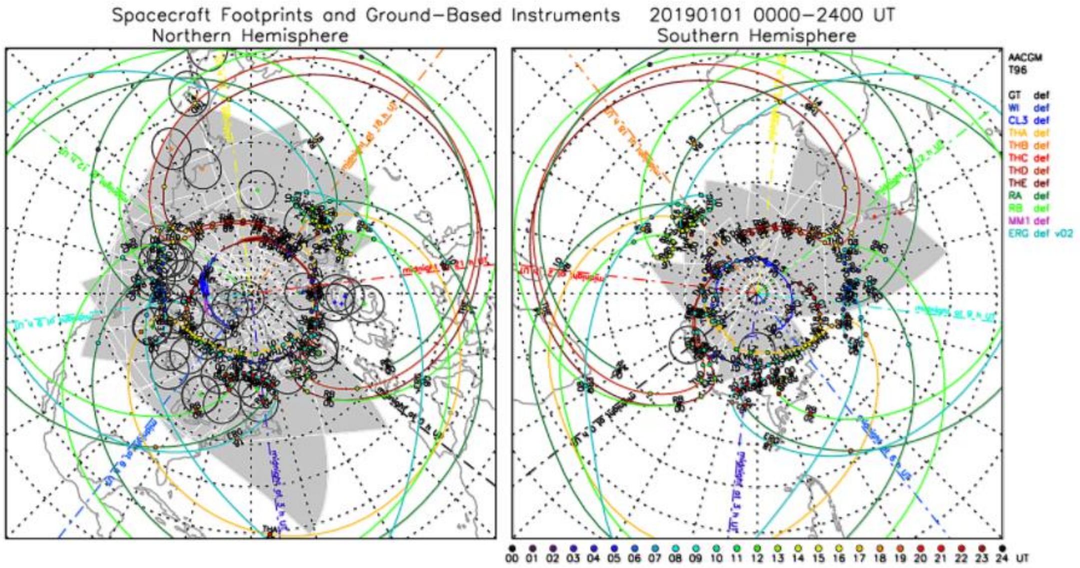

page 13, lines 12-16: The error caused by planarity or elongation of the tetrahedron could do with a clear statement that deformation remains low. If I have understood correctly, neither the standard curlometer technique nor the MRA method attempt to remove the error, and this could be clarified.

Response:

Yes, both these methods cannot remove the error caused by the tetrahedron. But for the result, we need to evaluate how big the error is, to guarantee it will not affect our analysis. We have clarified in line 4-5 in page 17 of the change-noted manuscript.

page 14, Figure 7: The caption should be improved - what are the red vertical lines in panels a and b? Apparently the cross-lines in panels c and d indicate the region applicable for these two events, but this could be clearly stated - it looks

like the panels were identical at first glance.

Response:

We have improved the caption, see line 2-4 in page 18 of the change-noted manuscript. The red vertical lines shown in panel a and b demarcate the concerned time interval for two events. The cross-lines in panels c and d is indeed very close, because for two events, Cluster is in the similar region and the tetrahedron shape is also similar. But there is also minor difference, which can be found in the lower horizon black line in panel c and d (see red box in the following Figure).

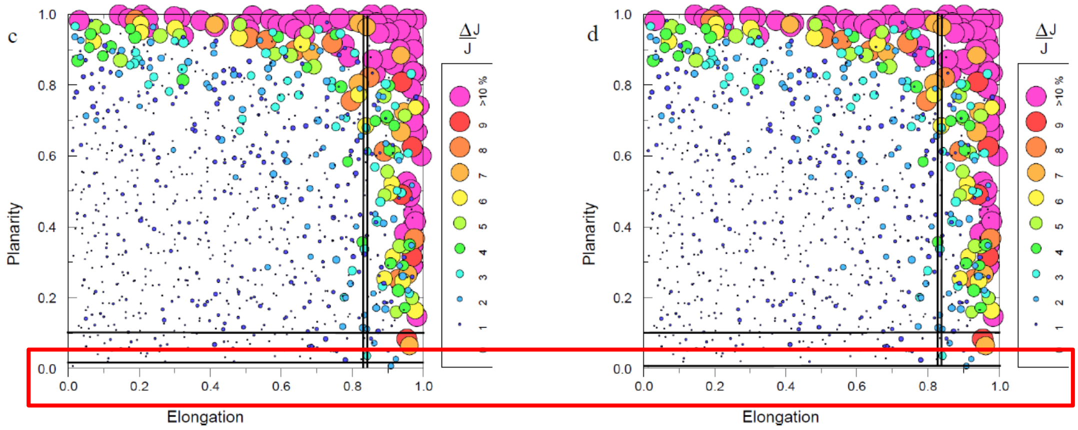

Technical corrections:

page 10 line 4: The reference is incorrectly formatted; it should read "De Michelis et al., 1999"

Response:

Modified. See line 4 in page 12 of the change-noted manuscript.

Strong Southward and Northward Currents Observed in the Inner Plasma Sheet

YanYan Yang[1, 2], Chao Shen[3], and Yong Ji[4]

[1]Institute of Crustal Dynamics, China Earthquake Administration, Beijing, 100085, China

[2]Center for Satellite Application in Earthquake Science, China Earthquake Administration, Beijing, 100085, China~~Key Laboratory of Crustal Dynamics, China Earthquake Administration, Beijing, 100085, China~~

[3]Harbin Institute of Technology, Shenzhen, 518055, China

[4]Department of Mechanics and Engineering Science, Peking University, Beijing, 100871, China

Correspondence to: Chao Shen (Email: shenchao@hit.edu.cn)

Abstract. It is generally believed that field aligned currents (FACs) and the ring current (RC) are two dominant parts of the inner magnetosphere. However, using the Cluster spacecraft crossing of the pre-midnight inner plasma sheet in the latitude region between 10 °N and 30 °N, it is found that, during ~~large storm events~~intense geomagnetic storms, in addition to FACs and the RC, there also exist strong southward and northward currents, which ~~cannot~~ should not be FACs, because the magnetic field in these regions is mainly along the *XY* plane. Detailed investigation shows that both magnetic field lines (MFLs) and currents in these regions high~~ly~~ ~~fluctuate~~dynamic. When the curvature of MFLs changes direction in the *XY* plane, the current also alternatively switches between southward and northward. Further analysis of the current generation mechanism indicates that the most reasonable candidate for the origin of these southward and northward currents is the curvature drift of energetic particles.

1 Introduction

Abundant current systems existing in the Earth's magnetosphere play a very important role in energy transformation in different regions (Kuijpers et al., 2014). Recently, through simulations and observations, numerous studies have shown that the inner magnetosphere currents have a more complicated structure and distribution than originally thought. For example, in the low latitude, the magnetic field geometry can be altered significantly into tail-like during storm time (Tsyganenko et al. 2003); One or multi banana current can exist in the inner magnetosphere, which makes the link of the current systems more complicated (Liemohn et al. 2013). In the high latitude, field-aligned currents (FACs) have more sophisticated structures except the known large scale region 1 and region 2 currents (Mishin et al., 1997; ~~Tsyganenko et al. 2003; Liemohn et al. 2013;~~ Dunlop et al., 2015a; 2015b). Therefore, more work is still needed to reveal the true nature of these current systems.

The huge progress in satellite deployments makes it possible for direct observation of the inner magnetosphere current system. It is believed that the magnetosphere and ionosphere are linked through a ring current (RC) and ~~field-aligned currents (~~FACs~~)~~ (e.g., Le et al. 2004; Zhang et al. 2011). Therefore, many investigations are mainly focused on these two current systems~~, respectively~~, from high ~~latitude~~ (e.g., Iijima and Potemra 1976; 1978; Wang et al., 2006; Dunlop et al., 2015b) and low latitude, respectively (e.g., Vallat et al. 2005; Shen et al. 2014; Yang et al. 2016). The region from low to middle latitude, which is the key area for the inner magnetosphere current link, however, has received less attention. Cartoon plots and some statistical results (e.g., Le et al., 2004) show that FACs should be the dominant current in these areas. Through Cluster satellite observations, Vallat et al. (2005) pointed out that the RC could exist at middle (or even high) latitudes. Despite the results achieved by these various research efforts, so far, there are still no findings enabling a conclusion about the complete current morphology in low and middle latitudes. For example, are FACs and the RC the only currents in these regions? If there are other currents, what is the corresponding generation mechanism for them? To address these questions, the current distribution and magnetic field geometry during two storm events are investigated in the latitude regions from 10 °N to ~~50~~30 °N.

In the following, we will use Cluster fluxgate magnetometer (FGM) (Balogh et al., 1997) data to conduct the analysis for two reasons: 1. the polar orbit of Cluster offers an opportunity to go through both the low-latitude and middle-latitude regions and 2. ~~the~~ The configuration of the four Cluster satellites makes it possible to ~~directly~~ calculate the current via Maxwell-Ampère's law and obtain the magnetic field geometry. Moreover, in many previous works, it was thought that an asymmetric RC linked with the FACs, which is generally believed to occur during storm time, so storm events are our primary focus here.

Throughout this paper, solar magnetospheric (SM) coordinates are used. To better describe angles, spherical coordinates (θ, ϕ) in the SM frame are also defined, i.e., the polar angle θ ($0° \leqslant \theta \leqslant 180°$) is the angle between the + *Z* axis and the vector direction while the azimuthal angle ϕ ($0° \leqslant \phi \leqslant 360°$) is anticlockwise rotated from the + *X* axis in the *XY* plane when seen from + *Z* axis. For current density analysis, the local cylindrical coordinate system (j_ρ, j_φ, j_z) (Vallat et al. 2005) is also utilized. Where j_z is parallel to the +Z axis; j_ρ represents the radial component of the current on the plane parallel to the X-Y plane, oriented anti-earthward; j_φ points eastward, describing RC.

2 Methodology

In this study, magnetic curvature analysis (MCA) (Shen et al., 2003) and magnetic rotation analysis (MRA) (Shen et al., 2007) are used; these techniques have the unique ability to reveal the three-dimensional geometric structure of the magnetic

域代码已更改
域代码已更改
域代码已更改
域代码已更改
带格式的: 字体: (中文) +中文正文 (宋体), 10 磅
带格式的: 字体: (中文) +中文正文 (宋体), 10 磅
带格式的: 字体: (中文) +中文正文 (宋体), 10 磅
域代码已更改
带格式的: 字体: (中文) +中文正文 (宋体), 10 磅
域代码已更改
带格式的: 字体: (中文) +中文正文 (宋体), 10 磅
带格式的: 字体: (中文) +中文正文 (宋体), 10 磅

field directly as well as provide more detailed magnetic-field-related parameters, such as magnetic field gradient, curvature, and the binormal of magnetic field lines, rotation rates, and current density. The magnetic unit vector $\hat{\mathbf{b}} = \mathbf{B} / |\mathbf{B}|$, curvature vector $\vec{\rho}_c$ ($\vec{\rho}_c = (\hat{\mathbf{b}} \cdot \nabla)\hat{\mathbf{b}}$), and the binormal vector $\hat{\mathbf{N}}$ ($\hat{\mathbf{N}} = \hat{\mathbf{b}} \times \hat{\boldsymbol{\rho}}_c / |\hat{\mathbf{b}} \times \hat{\boldsymbol{\rho}}_c|$) are orthogonal to each other in the analysis, and the radius of curvature is $R_c = 1/\rho_c$. The magnetic vector $\mathbf{b}$ has maximum, median, and minimum rotation rates of $\mu_1^{1/2}$, $\mu_2^{1/2}$, and $\mu_3^{1/2}$ along $\hat{\mathbf{e}}^{(1)}$, $\hat{\mathbf{e}}^{(2)}$, and $\hat{\mathbf{e}}^{(3)}$, respectively, where $\hat{\mathbf{e}}^{(1)}$, $\hat{\mathbf{e}}^{(2)}$, and $\hat{\mathbf{e}}^{(3)}$ are the three characteristic eigenvectors of the magnetic field. Note that, because the strong geomagnetic field in the region of interest will produce artificial currents in the basic MRA calculation (nonlinear contributions), the ~~International Geomagnetic Reference Field (IGRF)~~dipole field is subtracted when using the MRA method to minimize truncation error (Shen et al., 2014).

To make a comparison with the nondisturbed geomagnetic field, the local dipolar values of magnetic field strength B_{tDip}, radius of curvature, R_{cDip}, magnetic field gradient strength $|\nabla B_{Dip}|$, and three rotation rates $\mu_1^{1/2}$, $\mu_2^{1/2}$, and $\mu_3^{1/2}$ are also presented. They are calculated (Shen et al., 2014) by using:

$$
\begin{aligned}
& B_{tDip} = Mr^{-3}\sqrt{(1+3\cos^2\theta)}, \\
& R_{cDip} = \frac{r}{3}\sqrt{(1+3\cos^2\theta)^3} / [|\sin\theta| \cdot (1+\cos^2\theta)], \\
& |\nabla B_{Dip}| = 3\mathrm{M}r^{-4} \cdot \sqrt{1+\cos^2\theta(7+8\cos^2\theta)} / \sqrt{(1+3\cos^2\theta)}\ , \\
& \mu_1^{1/2} = \mu_\theta^{1/2} = 3(1+\cos^2\theta) / [r(1+3\cos^2\theta)], \\
& \mu_2^{1/2} = \mu_\phi^{1/2} = 3|\cos\theta| / [r\sqrt{(1+3\cos^2\theta)}], \\
& \mu_3^{1/2} = \mu_r^{1/2} = 0,
\end{aligned}
\qquad (1)
$$

where $M = m \cdot \mu_0 / 4\pi$ (with $m = 7.78 \times 10^{22}\ \mathrm{A \cdot m^2}$ being the earth's magnetic dipole moment) and r is the radial distance in SM coordinates.

3. Event Analysis

The chosen events occurred, respectively, on 12 April 2001 and 31 March 2001. These were the two largest storms from 2001 to 2004 during which the four Cluster satellites had a small (best) tetrahedron separation distance (≤1000 km). The minimum Dst indexes for the two events were −271 and −387 nT, respectively. During the two events, Cluster was in the pre-midnight sector and traversed the RC region vertically from the southern to northern hemispheres. The region of interested is in the northern hemisphere. Figure 1 gives the proton density and differential flux for H^+, He^+, O^+ during the concerned interval, which are obtained from Cluster Ion Spectrometer (CIS, Rème et al., 2001). The figure indicates that Cluster is mainly in plasma sheet region (e.g., Vallat et al. 2005).

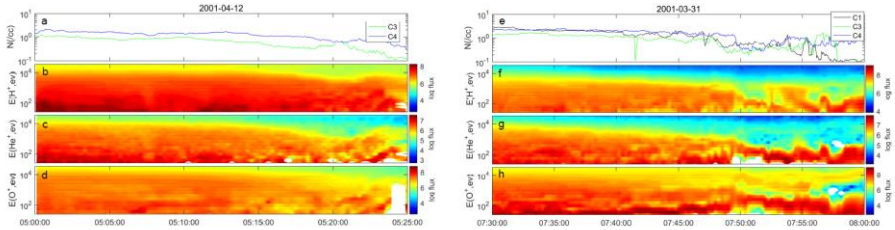

Figure 1: Cluster CIS data for 12 April 2001 (left) and 31 March 2001 (right) event. (a, e) the proton density variation for three satellites C1 (black), C3 (green) and C4 (blue). (b-d, f-h) H^+, He^+, O^+ energy time spectrograms in particle flux units ions/(cm2 sr s Kev) from C4.

3.1 12 April 2001 event

The time interval of interest for the first event is from 05:00 to 05:25 UT, with latitude ranging from 16.9° to 25.7°. Figure 2 presents some of the main physical quantities. Figure 2a shows the average magnetic field $\langle B_t \rangle$ detected from the four Cluster satellites and the local dipolar magnetic field strength. It can be seen that the local magnetic field is enhanced in this area. Figure 2b indicates that the polar angle of the magnetic field is close to 90°, indicating that the magnetic field lies approximately in the *XY* plane. The polar angle and azimuthal angle of dipolar fields is also show in dashed lines in Figure 2b, which indicates a large deviation of the azimuthal angle with observations. Figure 2c shows that the radius of curvature, R_c, has large variations. It is interesting to see that ϕ_c (the angle of R_c in Figure 2d) changes direction alternately during the whole period. Therefore, eight regions (numbered from NH1 to NH8) were chosen according to the changes in ϕ_c direction to investigate their features. The variations of some physical quantities are also summarized in Table 1. For ϕ_c and θ_{e1}, the average values (with a few large abnormal points removed) during this period is given. '-' denotes that the value has large oscillations. For j_z, the maximum or minimum value during each interval is presented.

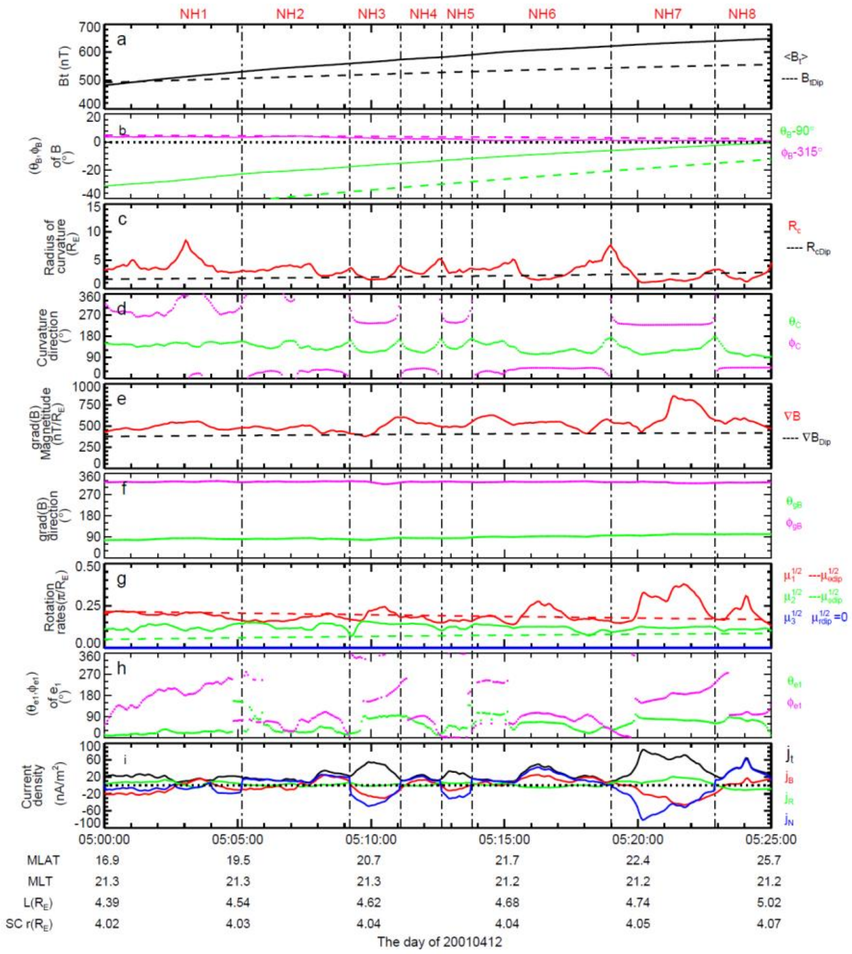

NH1
NH2
NH3
NH4
NH5
NH6
NH7
NH8
Bt (nT)
Radius of curvature (RE)
Curvature direction (°)
grad(B) Magnetitude (nT/RE)
grad(B) direction (°)
Rotation rates(π/RE)
Current density (nA/m²)
05:00:00
05:05:00
05:10:00
05:15:00
05:20:00
05:25:00
MLAT 16.9 19.5 20.7 21.7 22.4 25.7
MLT 21.3 21.3 21.3 21.2 21.2 21.2
L(RE) 4.39 4.54 4.62 4.68 4.74 5.02
SC r(RE) 4.02 4.03 4.04 4.04 4.05 4.07
The day of 20010412

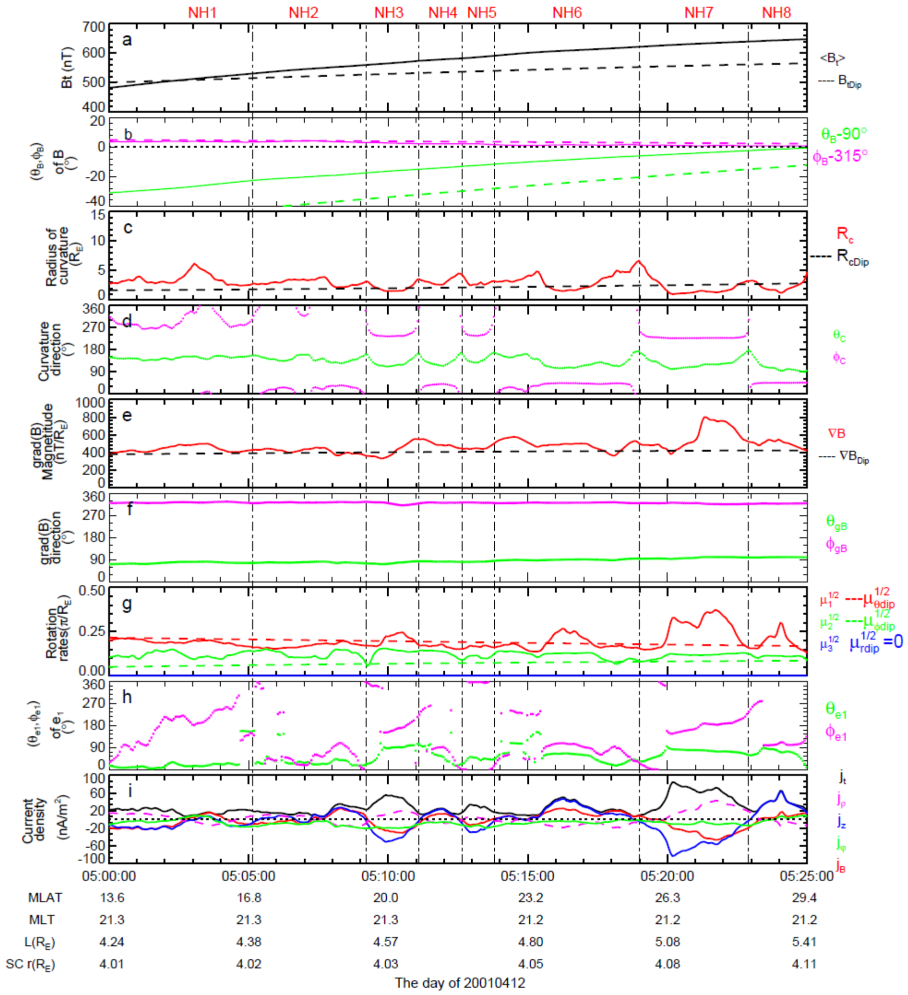

Figure 2: Geometry of the magnetic field and the current distribution in the NH region on 12 April 2001. (a) Average magnetic strength B_t at the center of the Cluster tetrahedron (black solid line) and the calculated strength B_{tDip} of the dipole geomagnetic field (black dashed line). (b) Direction angles (θ_B, ϕ_B) of the magnetic field. 90° and 315° are reduced respectively for θ_B and ϕ_B to better indicate the magnetic field variation. The polar angle and azimuthal angle of dipolar fields is also show in dashed lines. (c) Radius of curvature, R_c (red solid line), and the calculated radius of curvature, R_{cDip}, of the dipole geomagnetic field (black dashed line). (d) Direction angles (θ_c, ϕ_c) of the curvature of the MFLs. (e) Value of the gradient of magnetic field strength for the real magnetic field (red solid line) and dipole geomagnetic field (black dashed line). (f) Direction angles (θ_{gB}, ϕ_{gB}) of the gradient of magnetic field strength. (g) Maximum, median, and minimum rotation rates of the measured magnetic field (solid lines)

带格式的: 字体: (默认) Times New Roman, 10 磅

带格式的: 缩进: 首行缩进: 5.1 字符

and dipole geomagnetic field (dashed lines). (h) Direction angles (θ_{e1}, ϕ_{e1}) of the maximum rotation rate. (i) Total current density j_t (black line) and the three components j_ρ (magenta line), j_φ (green line), j_z (blue line) – in local cylindrical coordinate system, respectively. The red line is the field-aligned component j_B (red line).~~and the three components (j_B, j_R, j_N) of the current density at the local natural coordinates, where j_B is the field aligned component (red line), j_R the component along the curvature (green line), and j_N along the binormal. If the polar angle of j_N is smaller than 90°, then j_N is along northward, otherwise, it is along southward.~~

As shown in Figure 2c, the radius of curvature of MFLs in the eight regions is ~~basically decreased~~varied compared with that of the dipole field. Another feature observed in Figure 2c is that R_c peaks at the vertical dashed lines. It is reasonable since the curvature radius in transition region should be larger than the region where the curvature radius has opposite directions. Figure 2d and ϕ_c row in Table 1 give the average value of the azimuthal direction ϕ_c during each interval. It quantitatively reveals that ϕ_c alternatively varied between 30.3°–51.9° and 230.3°–292.0°. It is noted from Figure 2d that, for some regions, the variation of polar angle θ_c has larger fluctuation (than azimuthal angle ϕ_c). This feature reflects larger changes of the magnetic field in Z component. Figure 2g shows that $\mu_1^{1/2}$ has an enhancement in each region, illustrating a stretched MFL structure. Figure 2h and row θ_{e1} in Table 1 show that, for most regions, the largest value of the polar angle θ_{e1} for $\mu_1^{1/2}$ is close to 90°; therefore, the largest deviation of MFLs is along the *XY* plane. Figure 2i indicates that the current oscillates and that the dominant current is along j_ρ ~~the MFLs j_B~~ and north (or south) j_z ~~j_N~~ direction, while ~~the current along the curvature j_R~~ – ~~i~~ j_φ is basically small compared with j_ρ ~~j_B~~ and j_z ~~j_N~~. – To show FACs, j_B component is also given in Figure 2i, it can be seen that the value of j_B close to that of j_ρ, because the direction of the magnetic field points approximately to the radial direction (see Figure 2b). The maximum values for j_B and j_z ~~j_N~~ were ~~~50~~ 40 and ~80 nA/m^2, respectively. From Table 1 and Figure 2, it is interesting to see that, from region NH1 to region NH8, the j_z ~~j_N~~ component changed from positive (northward) to negative (southward) as ϕ_c varied from <~~60~~50° to >230°.

Table 1: Variation of physical quantities for two storm events

带格式的: 字体: 小五, 加粗, 字体颜色: 黑色
域代码已更改
带格式的: 字体: 小五, 加粗, 字体颜色: 黑色
域代码已更改
域代码已更改
带格式的: 字体: 小五, 加粗
带格式的: 字体: 小五, 加粗
域代码已更改
带格式的: 字体: (默认) +西文正文 (Calibri), (中文) +中文正文 (宋体), 五号, 字体颜色: 自动设置
域代码已更改
域代码已更改
域代码已更改
域代码已更改
域代码已更改
带格式的: 字体: 非倾斜, 非升高量 / 降低量
域代码已更改
域代码已更改
域代码已更改
域代码已更改
域代码已更改

Event[a]	PQ[b]	NH1[c]	NH2[d]	NH3[e]	NH4[f]	NH5[g]	NH6[h]	NH7[i]	NH8[j]	NH9[k]	NH10[l]	NH11[m]
20010412	ϕ_c (°)	292.0	41.4	244.1	35.3	251.9	36.9	230.3	44.8			
	θ_{e1} (°)	29.5	27.0	74.7	57.7	51.9	61.0	70.8	69.7			
	j_{zm} (nA/m^2)	419.3	25.327.	49.3-	-21.523	30.9-	-43.146	81.8-	-61.963			
	j_{Nm} (nA/m^2)	-22.5	2	50.8	.3	28.8	.6	82.6	.1			
20010331	ϕ_c (°)	59.9	241.9	59.6	244.7	58.5	240.3	63.2	235.1	60.5	238.6	62.8
	θ_{e1} (°)	71.3	-	65.4	73.2	71.8	59.8	73.4	71.7	78.8	59.9	80.2
	j_{zm} (nA/m^2)	106.9	−42.5=	60.15	−128.3	95.99	−126.3	198.2	−294.3	118.2	−193.9	204.720
		95.6	45.9	6.1	−125.6	8.0	−123.8	225.6	−328.9	118.9	−202.4	4.4

[a]Storm events considered in this work.

[b]The physical quantity ϕ_c is the average azimuthal direction of the curvature radius, θ_{e1} is the average polar angle of maximum rotation rates of the magnetic field, and j_{zm} represents the maximum or minimum value of the j_z current component.

[c–m]Regions for each storm event.

3.2. 31 March 2001 event

Another larger storm occurred between 07:30 and 08:00 UT on 31 March 2001. (The event was once reported by Shen et al. (2014), but they only concentrated on the interval from ~07:00 to 7:25 UT). Observations are shown in Figure 3 for the latitude region from 13.1 °N to 3431.62 °N, the interval during the main phase of the storm. Here, 11 regions designated from NH1 to NH11 are divided also according to azimuthal direction changes of ϕ_c. The variations of some relative physical quantities are also shown in Table 1. From Figure 3 and Table 1, it can be seen that these parameters behave the as same as those that of the 12 April 2001first event, but with strong magnetic field strength. Figure 3 indicates that the magnetic field strength is stronger than that during the first event. The magnetic field is in the *XY* plane (see Figure 3b). The radius of curvature of MFLs (see Figure 3c), the magnetic field gradient (Figure 3e), a. And the largest rotation rate (Figure 3g) oscillates significantly and exhibits large deviations compared with those of the dipole field. Figure 3f shows that the magnetic field gradient is in the *XY* plane and directed toward the dayside. Figure 3h and row θ_{e1} demonstrate that the

域代码已更改
带格式的: 字体: 10 磅
带格式的: 字体: Times New Roman, 10 磅
带格式的: 字体: Times New Roman
带格式的: 字体: 10 磅
带格式的: 字体: Times New Roman, 10 磅
带格式的: 字体: 10 磅
带格式的: 字体: Times New Roman, 10 磅
带格式的: 字体: 10 磅
带格式的: 字体: Times New Roman, 10 磅
带格式的: 字体: 10 磅
带格式的: 字体: Times New Roman, 10 磅
带格式的: 字体: 10 磅
带格式的: 字体: Times New Roman
带格式的: 字体: Times New Roman
带格式的: 字体: Times New Roman
带格式的: 字体: Times New Roman

largest variation of MFLs is near the *XY* plane. In Figure 3i, it is clear that the j_z ~~j_N~~ component is the dominant current, with a maximum value of ~300 nA/m^2. This value is more than triple that of the 12 April 2001 event. It is clear to see that the j_φ ~~j_R~~ component is the smallest among these currents. Similar to first event, j_z ~~j_N~~ is simultaneously observed to vary from northward to southward when φ_c changes direction.

域代码已更改

域代码已更改

域代码已更改

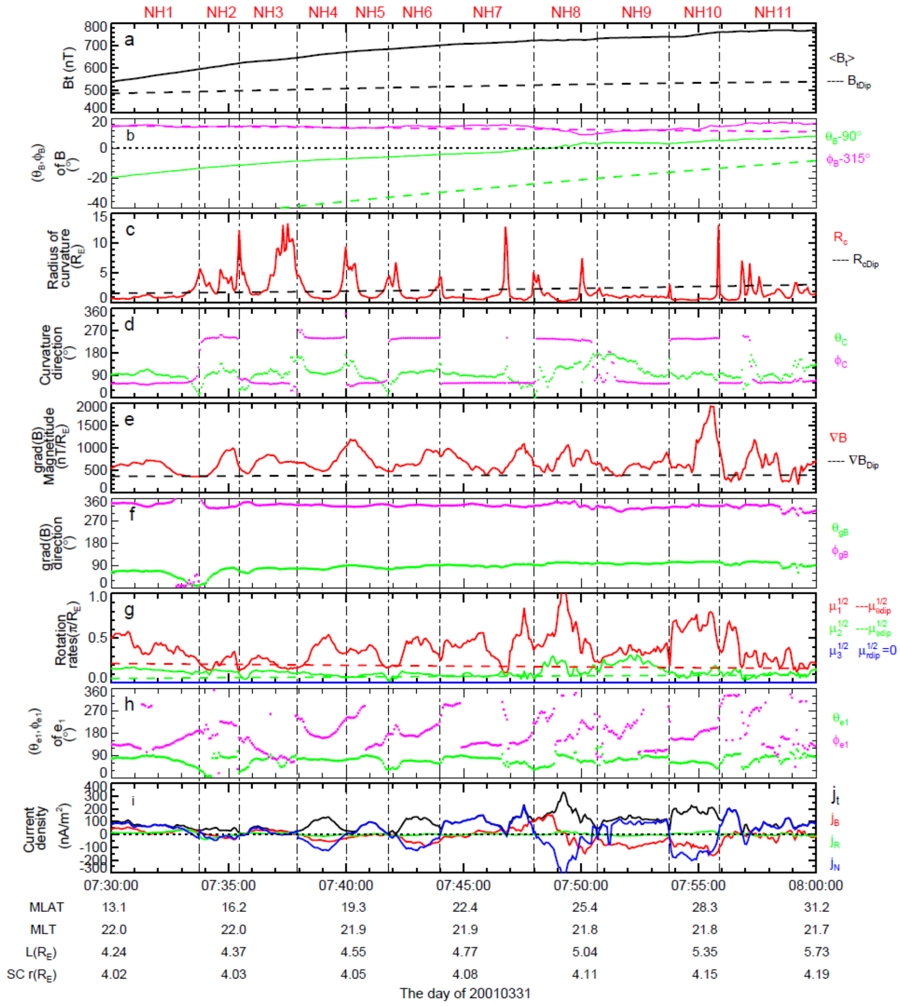

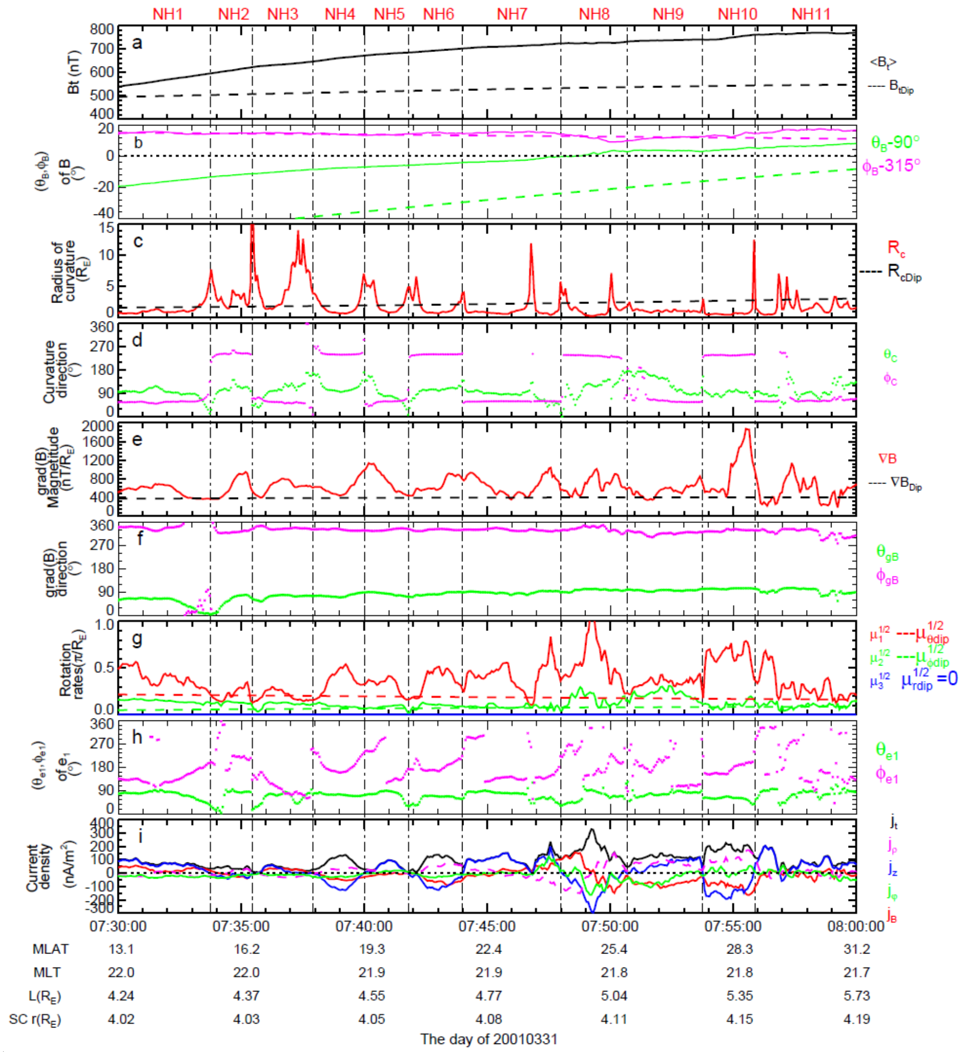

Figure 3: Geometry of the magnetic field and the current distribution in the NH region on 31 March 2001. The format is the same as that of Figure 2.

带格式的: 字体: (默认) Times New Roman, 10 磅, 加粗

带格式的: 缩进: 首行缩进: 3.99 字符

4 ~~Summary and~~ Discussion

During the 12 April 2001 and 31 March 2001 strong storm events, the Cluster satellites were located in the pre-midnight sector and crossed from ~13.10 °N to 42.6~30 °N. In these regions, both the magnetic field parameters and the current density fluctuated significantly. The MFLs, which were mainly in the *XY* plane, severely deviated from the dipole field and changed (stretched) along the *XY* plane. Figure 4 displays the total magnetic field strength and its three components. It can be seen that the *X* and *Y* components of the magnetic field have the largest fluctuations, which is consistent with the results obtained from Figure 2 and 3. To further investigate the fluctuation, the continuous 1-D wavelet transform method is applied in X and Y component of the magnetic field. It is found that the ULF wave covering a range of frequencies spanning 4 mHz to 10 mHz can be observed (not shown here), which is consistent with the typical current density variation in ~2-4min period. Actually, ULF wave in the plasma sheet region has been extensively reported in previous works (see Keiling, 2009 and references therein). So, it seems that ULF wave is a possible way to cause the variation of curvature radius (and the field aligned current).

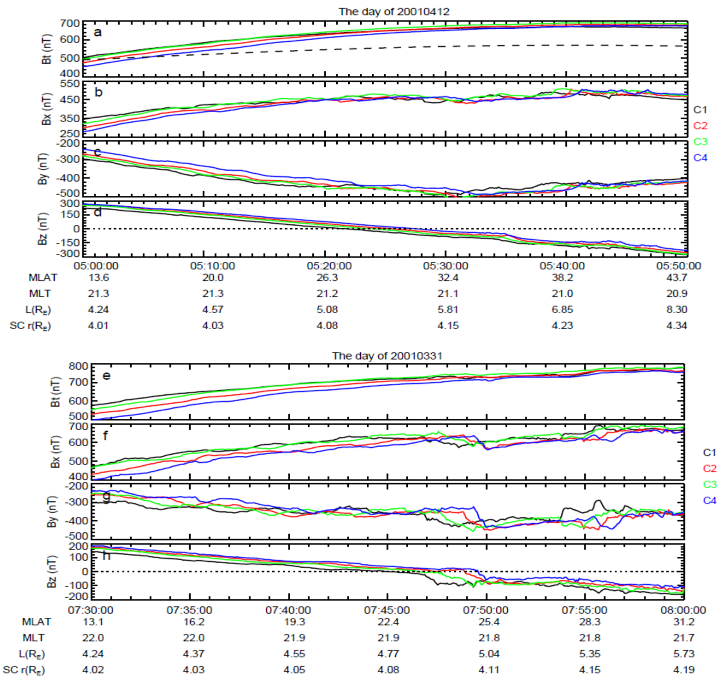

Figure 4: Magnetic field observed by the four Cluster spacecraft during 12 April 2001 and 31 March 2001 storm events.

The most obvious phenomenon in the two cases is that the existence of three current systems, i.e., FACs j_B, an azimuthal current ~~(RC)~~ j_φ ~~j_R~~ and a northward (or southward) current j_z ~~j_N~~. Among them, j_z ~~j_N~~ is basically the strongest current component. In previous studies (e.g., Le et al., 2004; Vallat et al., 2005), the existence of j_B and j_φ ~~j_R~~ has been proved. However, the occurrence of such a strong j_z ~~j_N~~ in the inner plasma sheet has not been reported before. In the work of Vallat et al., (2005), they also found a southward current (see Fig 14 and corresponding text). But it is in equatorial ring current region (with no direction changes) and mainly caused by an asymmetry between the ionospheric conductivities of the

域代码已更改
域代码已更改
域代码已更改
域代码已更改
域代码已更改

two hemispheres. It is very clear that the southward current in their paper is different with what we report here.

As introduced in previous studies (e.g., Parker, 1957), the current in the inner magnetosphere generally arises from gradient drifts as well as curvature drift and the gyromotion of energetic particles. They can be calculated by using (e.g., Lui et al., 1987; De Michelis et al., 1999):

$$\mathbf{j}_{\nabla} = P_{\perp}\frac{\mathbf{B}\times\nabla B}{B^3}, \quad (2)$$

$$\mathbf{j}_{C} = -\frac{P_{\parallel}}{B^2}\boldsymbol{\rho}_{\mathbf{c}}\times\mathbf{B}, \quad (3)$$

$$\mathbf{j}_{G} = \frac{\mathbf{B}}{B^2}\times\left[\nabla P_{\perp} - \frac{P_{\perp}}{B}\nabla B - \frac{P_{\perp}}{B^2}(\mathbf{B}\cdot\nabla)\mathbf{B}\right], \quad (4)$$

where $\mathbf{j}_{\nabla}$, $\mathbf{j}_{C}$, and $\mathbf{j}_{G}$ represent the gradient current, curvature current, and gyromotion current, respectively, and $P_{\perp}$ $P_{\parallel}$ are the pressure tensor components perpendicular and parallel to the magnetic field, which can be deduced from:

$$P_{\perp} = \pi\sqrt{2\mathrm{m}}\iint J\sqrt{\varepsilon}\sin^3\alpha\, d\alpha\, d\varepsilon, \quad (5)$$

$$P_{\parallel} = 2\pi\sqrt{2\mathrm{m}}\iint J\sqrt{\varepsilon}\cos^2\alpha\sin\alpha\, d\alpha\, d\varepsilon, \quad (6)$$

where m is mass of particle, J is the differential flux intensity, ε and α ~~is respectively~~are the particle energy and pitch angle, respectively. Since the magnetic field gradient ∇B and curvature $\boldsymbol{\rho}_{\mathbf{c}}$ have been obtained by using MRA method, the above three currents can be calculated when the pressure tensor components are given.

For the two events in this study, both the magnetic field and magnetic field gradient are directed toward the dayside. Therefore, the current deduced from $\mathbf{B}\times\nabla B$ (the gradient drift current) should be small. To analyze the current contribution from gyromotion drift and curvature drift, we first show the three components of $-\boldsymbol{\rho}_{\mathbf{c}}\times\mathbf{B}$ for the two events in Figure 5a and 5b. It is clearly seen that the $(-\boldsymbol{\rho}_{\mathbf{c}}\times\mathbf{B})_z$ component is the dominate part and has the same variation trend with j_z. Therefore, the curvature drift current is a possible candidate. For gyromotion current, it is originated from three terms, i.e., $\mathbf{B}\times\nabla P_{\perp}$, -$\mathbf{B}\times\nabla B$ and -$\mathbf{B}\times(\mathbf{B}\cdot\nabla)\mathbf{B}$. Firstly, according to previous works (e.g., Lui et al., 1987; De Michelis et al., 1999), $\nabla P_{\perp}$ is along the radial direction, which means that it has the similar direction with magnetic field for two

域代码已更改

域代码已更改

域代码已更改

域代码已更改

域代码已更改

域代码已更改

域代码已更改

events concerned here. So, the contribution from $\mathbf{B}\times\nabla P_{\perp}$ should be small. Secondly, $-\mathbf{B}\times\nabla B$ is similar to the gradient drift current and can be negligible. Thirdly, since $(\mathbf{B}\cdot\nabla)\mathbf{B}$ has the same direction with ρ_c ($\rho_c=(\hat{\mathbf{b}}\cdot\nabla)\hat{\mathbf{b}}, \hat{\mathbf{b}}=\mathbf{B}/|\mathbf{B}|$), according to Figure 5a and 5b, the product of $-\mathbf{B}\times(\mathbf{B}\cdot\nabla)\mathbf{B}$ (similar to $\rho_c\times\mathbf{B}$) will behave oppositely to j_z. Consequently, the gyromotion current has little possibility of contributing to a strong j_z. Figures 5a and 4b show the $-\rho_c\times\mathbf{B}$ result for the two events. It is clearly seen that the $-(\rho_c\times\mathbf{B})_z$ component has the same variation trend as j_z. For the gyromotion contribution, because $\nabla P_{\perp}$ is generally believed to be along the *Z* direction, $\mathbf{B}\times\nabla P_{\perp}$ should be in the *XY* plane. $-\mathbf{B}\times\nabla B$ is similar to the gradient drift current and should be small. According to the $-\rho_c\times\mathbf{B}$ result in Figure 5, $\rho_c\times\mathbf{B}$ behaves oppositely to j_z. Consequently, the gyromotion current has little possibility of contributing to a strong j_z and According to the above analysis, the most reasonable candidate for strong j_z should be the curvature drift.

Based on the above analysis, cartoon plots are given in Figures 5c and 5d to explain the possible generation mechanism for j_z. During the strong storm time, turbulent turbulences, (e.g., ULF waves,) result to in the fluctuation of the MFLs, then, the radius of curvature of the MFLs decreases, leading to an increase in the curvature drift current. During this process, the direction of the magnetic field is nearly unchanged because the background field is very strong. However, the curvature will alternately change directions along with the variation of the MFLs, resulting in alternating variations of $-\rho_c\times\mathbf{B}$, i.e., leading to the oscillation of j_z.

域代码已更改

域代码已更改

域代码已更改

域代码已更改

域代码已更改

域代码已更改

域代码已更改

域代码已更改

域代码已更改

域代码已更改

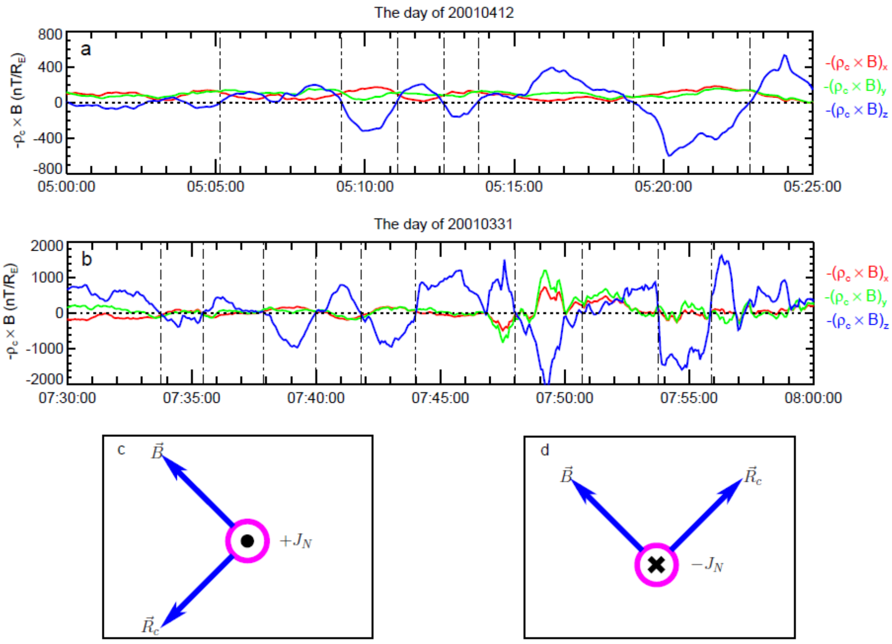

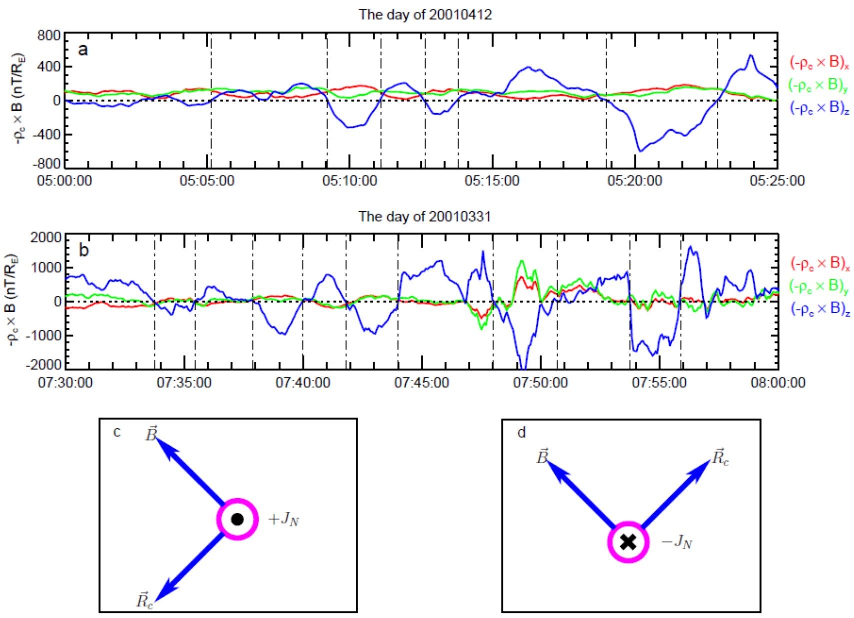

Figure 5: (a) and (b) The three components of $-\rho_c \times \mathbf{B}$ for two concerned events. ρ_c is calculated from MRA method and $\mathbf{B}$ is the averaged magnetic field measured by four Cluster. ~~Results deduced from the radius of curvature of the cross magnetic field~~. (c) and (d) Cartoon plots of the origin of the j_N current variation.

带格式的: 字体: (默认) Times New Roman, 10 磅, 加粗

带格式的: 缩进: 首行缩进: 5.5 字符

域代码已更改

域代码已更改

域代码已更改

Figure 5 (a) and (b) can only illustrates that the direction of $-\rho_c \times \mathbf{B}$ is consistent with northward current. To quantitatively check if curvature current calculated through Eq. (3) is consistent with result obtained from MRA method, further investigation deserve to be tried. The CIS/CODIF (Composition and Distribution Function analyzer) can provide the differential flux intensity for energy below 40kev. Through Eq. (3) and (5, 6), the curvature current can be estimated. The result shows that the main variation trend is consistent with result from MRA, but the intensity is very small (less than 1 nA/m^2, not show here). However, it should be noted that, for Cluster CIS/CODIF, only low energetic particle data are available, therefore, large bias may exist when calculating storm time current. In contrast, much higher energy is used in previous studies (e.g., to 1Mev in the work of Lui et al., 1987). Cluster RAPID can provide energy spectrograms for high energetic particle from ~27.6kev to ~3056 kev. Unfortunately, there is no available data for the two concerned events. The statistical study from Kronberg et al. (2015) proves that, in the near earth plasma sheet, higher energetic hydrogen and oxygen are greatly enhanced during geomagnetic activity. In the work of Ma et al. (2012), they also indicated that the flux for higher energetic particles could comparable or larger than that of the low energetic particles.

Though, there is no available differential flux for high energetic particles on Cluster, the curvature current still can be estimated through simulations. Previous works has proved that the particle distribution in plasma sheet can be described as Kappa distribution functions (Pierrard and Lazar, 2010, and references therein):

$$\text{f}=N_1\left(\frac{1}{2\pi m E_0 \kappa_1}\right)^{2/3}\frac{\Gamma(\kappa_1+1)}{\Gamma(\kappa_1-1/2)}\left(1+\frac{E}{\kappa_1 E_0}\right)^{-\kappa_1-1} \quad (7)$$

Where N_1 and E_0 denotes to particle density and temperature, and κ_1 is a constant. For energy satisfying $E >> E_0$, Eq. (7) can be written as:

$$f = aE^{-\kappa_1-1} \quad (8)$$

Since the differential flux intensity J and particle velocity distribution function f is related by $J = fp^2$, Eq. (8) is also the function of J, namely:

$$J = ap^2 E^{-\kappa_1-1} \quad (9)$$

Where p is the momentum of the concerned particles, and a is a constant. Thus, with the known differential flux intensity from low energetic particle, the parameter a and κ_1 can be determined. Then, the differential flux intensity for high energetic particles (to 1Mev) can be estimated using Eq. (9). Though, particles are accelerated during the storm, we have confirmed that the Kappa distribution is still satisfied using CIS/CODIF observations (not shown here). However, it should be noted that, during the storm, a and κ_1 are no longer a constant but varied with time. Besides, to check if the estimated high energetic particle differential flux (using low energy particle data) is reasonable, we select a storm event occurred on 20 April 2002, which has similar position with two concerned events in this study, and has CIS/CODIF and RAPID observations at the same time. The result shows that the fitted result (from CIS/CODIF measurement) can basically reflect the main trend of the high energetic particles, which can demonstrate that our estimation used here is reasonable.

域代码已更改

域代码已更改

Now, we can re-estimate the curvature current using Cluster CIS/CODIF observations for energy between 25ev-40kev and simulation values for energy >40kev-1Mev. Figure 6 shows the estimated z component of curvature current (the red dotted curve). It is close to result from MRA (the blue curve).

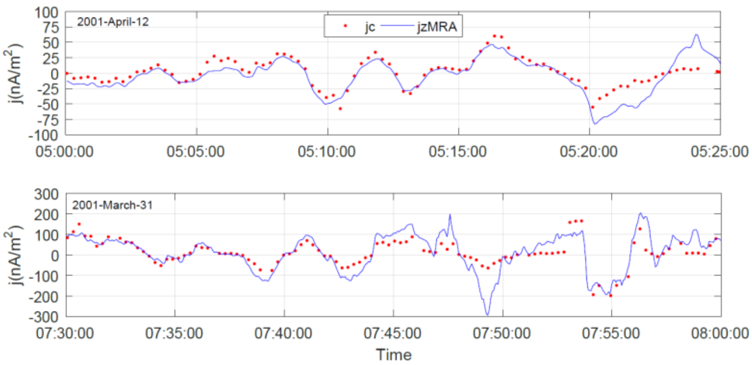

Figure 6: The z component current density calculated from MRA method (the blue curve) and the estimated curvature current (the red dotted curve).

It should be noted that both two events concerned here is in the north hemisphere. Actually, we have checked that the southward and northward current also can be observed in the southern low and middle latitudes. So, such currents should be observable both in north and south inner plasma sheet during strong geomagnetic storm events.

According to previous analysis from plasma data (Baker et al., 2002; Korth et al., 2004; Vallat et al., 2005; Ohtani et al., 2007), most NH regions should correspond to the plasma sheet region. Using the T96 model (Tsyganenko, 1995, 1996), we have tried to trace Cluster footprints in the northern hemisphere, it is found that ~~When the Cluster footpoint traces the T96 model,~~ the position is ~55 °–60 ° ~~in the northern hemisphere~~ (not shown here), which just corresponds to the position of the FACs (Papitashvili et al, 2002; He et al, 2012). Because the MFL shapes in the plasma sheet have been changed considerably, the particle motion in Earth's magnetic field will be altered correspondingly, which may affect the particle distribution in the polar and equatorial regions, hence, leading to the variation of the FAC and RC distributions. These effects, however, need to be evaluated in future work.

When calculate current density using MRA method, it should be noted that Cluster is not a regular tetrahedron shape around the perigee area, but suffers to an elongation, which can produce an unnatural currents. These unnatural currents are included in our analysis and cannot be removed. To evaluate this component, methods from Robert et al. (1998) and Vallat et al. (2005) are used. Figure 7 gives the Cluster tetrahedron parameters for two concerned events. Then, the current influence of the tetrahedron shape can be estimated as a function of elongation and planarity (Figure 7c and Figure 7d). It can be seen that the error caused by tetrahedron is never more than 30%.

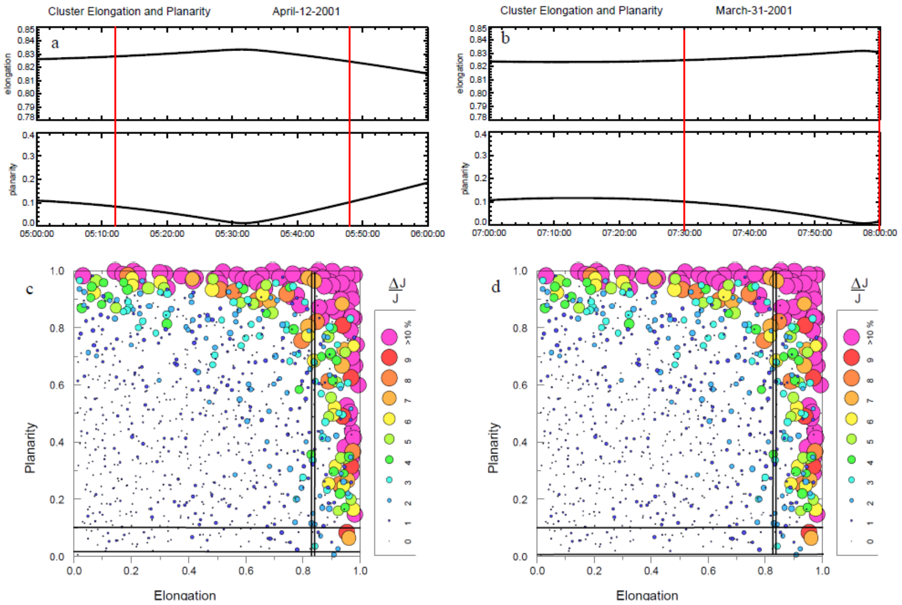

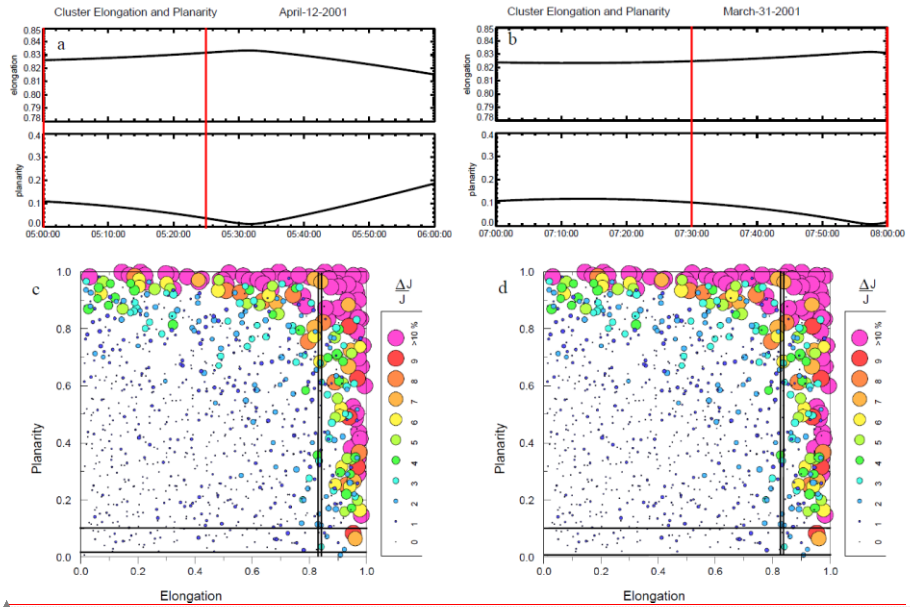

Figure 7: Panel a and b: Cluster elongation and planarity for two studied events. The red vertical lines ~~show~~ demarcate the concerned time interval. Panel c and d are picked from Robert et al. (1998) to evaluate the influence of the tetrahedron shape. Black lines mark the elongation and planarity obtained from panel a and b.

5 Sumamry

In this work, the magnetic field geometry and current density in the inner plasma sheet during two intense geomagnetic storms have been investigated. It is found that, the magnetic field and current density are highly fluctuated in this region. Generally, both three components of current can be observed during the concerned interval. However, the northward (or southward) current is basically the strongest one. Detailed study shows that, the MFLs line in XY plane, so, the northward (or southward) current should not be FACs. This property has not been reported before.

The most prominent feature of the northward (or southward) current is the alternative changing of its direction, which is found to vary simultaneously with that of the curvature. To reveal the generation mechanism of the northward (or southward) current, gradient current, curvature current, and gyromotion current are analyzed, respectively. The result shows that the curvature current has the same variation trend with the northward and southward current. Then, using low energetic particle observations from Cluster CIS/CODIF, combined with simulations based on Kappa distribution, the curvature current is calculated. It shows that the estimated curvature current coincides very well with the current density directly obtained from MCA and MRA. Therefore, the curvature drift of the energetic particle is the most reasonable mechanism of the southward and northward current.

带格式的：字体：(默认) Times New Roman, 10 磅

带格式的：缩进：首行缩进： 4.52 字符

带格式的：英语(美国)

带格式的：标题 1

For the two events concerned in this work, we can observe ULF waves, which is consistent with the typical current density variation period. These turbulences excited during the strong storm can result to the decrease of curvature radius and changing of direction of MFLs, then leading to an increase of the curvature currents and variation of their direction.

带格式的：正文，缩进：首行缩进：0.5 字符，行距：1.5 倍行距

带格式的：字体：10 磅

Acknowledgments and Data

This work was supported by National Key R&D Program of China (Grant no. 2018YFC1503501) and the National Natural Science Foundation of China (Grant Nos. 41874190, 41231066 and 41204117). Solar wind data (OMNI data set) were obtained from http://omniweb.gsfc.nasa.gov; Cluster FGM and CIS/CODIF data were obtained respectively from ftp://cdaweb.gsfc.nasa.gov/pub/data/Cluster/, https://www.cosmos.esa.int/web/csa.

References

Angelopoulos, V.: The THEMIS Mission, Space Sci. Rev., 141, 5–34, doi:10.1007/s11214-008-9336-1, 2008.

Baker D. N., R. E. Ergun, J. L. Burch, J.-M. Jahn, P. W. Daly, R. Friedel, G.D. Reeves, T.A. Fritz, and D. G. Mitchell: A telescopic and microscopic view of a magnetospheric substorm on 31 March 2001, *Geophys. Res. Lett.*, 29(18), 1862, doi:10.1029/2001GL014491, 2002.

Balogh, A., et al.: The Cluster magnetic field investigation, *Space Sci. Rev.*, 79(1–2), 65–91, doi:10.1023/a:1004970907748, 1997.

De Michelis, P., I. A. Daglis, and G. Consolini: An average image of proton plasma pressure and of current systems in the equatorial plane derived from AMPTE/CCE-CHEM measurements, *J. Geophys. Res.*, 104(A12), 28615–28624, doi:10.1029/1999JA900310, 1999.

Dunlop, M. W., J.-Y. Yang, Y.-Y. Yang, C. Xiong, H. Lühr, Y. V. Bogdanova, C. Shen, N. Olsen, Q.-H. Zhang, J.-B. Cao, H.-S. Fu, W.-L. Liu, C. M. Carr, P. Ritter, A. Masson, and R. Haagmans: Simultaneous field-aligned currents at Swarm and Cluster satellites. *Geophys. Res. Lett*., 42, 3683–3691. doi: 10.1002/2015GL063738, 2015a.

Dunlop, M. W, Y. Y. Yang, J.-Y. Yang, H. Lühr, C. Shen, N. Olsen, P. Ritter, Q.-H. Zhang, J.-B. Cao1, H.-S. Fu, and R. Haagmans: Multispacecraft current estimates atswarm, *J. Geophys. Res. Space Physics*, 120, 8307–8316, doi:10.1002/2015JA021707, 2015b.

He, M., J. Vogt, H. Lühr, E. Sorbalo, A. Blagau, G. Le, and G. Lu: A high-resolution model of field-aligned currents through empirical orthogonal functions analysis (MFACE), Geophys. Res. Lett., 39, L18105, doi:10.1029/2012GL053168, 2012.

Iijima, T., and T. A. Potemra: Field-aligned currents in the dayside cusp. observed by Triad. J. Geophys. Res., 81, 5971, doi:

10.1029/JA081i034p05971, 1976.

Iijima, T., and T. A. Potemra: Large-scale characteristics of field-aligned currents associated with substorms. J. Geophys. Res., 83, 599-615, doi: 10.1029/JA083iA02p00599, 1978.

Keiling, A.: Alfvén waves and their roles in the dynamics of the Earth's magnetotail: A review, Space Sci. Rev., 142(1 – 4), 73 – 156, doi:10.1007/s11214 - 008 - 9463 - 8, 2009.

Korth, A., et al.: Ion injections at auroral latitude during the March 31, 2001 magnetic storm observed by Cluster, Geophys. Res. Lett., 31, L20806, doi:10.1029/2004GL020356, 2004.

Kronberg, E. A., E. E. Grigorenko, S. E. Haaland, P. W. Daly, D. C. Delcourt, H. Luo, L. M. Kistler, and I. Dandouras: Distribution of energetic oxygen and hydrogen in the near-Earth plasma sheet, J. Geophys. Res. Space Physics, 120, 3415–3431, doi:10.1002/2014JA020882, 2015.

Kuijpers, J., H. Frey, and L. Fletcher: Electric Current Circuits in Astrophysics, Space Sci Rev, 1-55, 2014.

Le, G., C. T. Russell, and K. Takahashi: Morphology of the ring current derived from magnetic field observations, Ann. Geophys., 22,1267–1295, 2004.

Liemohn, M. W., N. Y. Ganushkina, R. M. Katus, D. L. De Zeeuw, and D. T. Welling: The magnetospheric banana current, J. Geophys. Res. Space Physics, 118, doi:10.1002/jgra.50153, 2013.

Lui, A. T. Y., R. W. McEntire, and S. M. Krimigis: Evolution of the ring current during two geomagnetic storms, J. Geophys. Res., 92(A7), 7459–7470, doi:10.1029/JA092iA07p07459, 1987.

Ma, Y., C. Shen, V. Angelopoulos, A. T. Y. Lui, X. Li, H. U. Frey, M. Dunlop, H. U. Auster, J. P. McFadden, and D. Larson: Tailward leap of multiple expansions of the plasma sheet during a moderately intense substorm: THEMIS observations, J. Geophys. Res., 117, A07219, doi:10.1029/2012JA017768, 2012.

Mishin, V. M., et al.: A study of the CDAW 9C substorm of May 3, 1986, using magnetograrn inversion technique 2, and a substorm scenario with two active phases, J. Geophys. Res., 102(A9), 19845–19859, doi:10.1029/97JA00154, 1997.

Ohtani, S., et al.: Cluster observations in the inner magnetosphere during the 18 April 2002 sawtooth event: Dipolarization and injection at r=4.6 RE, J. Geophys. Res., 112, A08213, doi:10.1029/2007JA012357, 2007.

Parker, E. N.: Newtonian development of the dynamical properties of ionized gases of low density, Phys. Rev., 107, 924–933, 1957.

Papitashvili, V. O., F. Christiansen, and T. Neubert: A new model of field-aligned currents derived from high-precision satellite magnetic field data, Geophys. Res. Lett., 29(14), 1683, doi:10.1029/2001GL014207, 2002.

Pierrard, V., and M. Lazar: Kappa distributions: Theory and applications in space plasmas, Sol. Phys., 267, 153–174, doi:10.1007/s11207-010-9640-2, 2010.

Rème, H., Aoustin, C., Bosqued, J., Dandouras, I., Lavraud, B., Sauvaud, J. A., Barthe, A., Bouyssou, J., Camus, Th., Coeur-Joly, O., et al.: First multispacecraft ion measurements in and near the Earth's magnetosphere with the identical Cluster ion spectrometry (CIS) experiment, Ann. Geophys., 19, 1303–1354, 2001.

Robert, P., Dunlop, M. W., Roux, A., and Chanteur, G (1998): Accuracy of current density determination, in Analysis Methods for Multi-Spacecraft data, ISSI Sci. Rep. SR-001, 395–418.

Shen, C., X. Li, M. Dunlop, Z. X. Liu, A. Balogh, D. N. Baker, M. Hapgood, and X. Wang: Analyses on the geometrical structure of magnetic field in the current sheet based on cluster measurements, J. Geophys. Res., 108(A5), 1168, doi:10.1029/2002JA009612, 2003.

Shen, C., X. Li, M. Dunlop, Q. Q. Shi, Z. X. Liu, E. Lucek, and Z. Q. Chen: Magnetic field rotation analysis and the applications, J. Geophys. Res., 112, A06211, doi:10.1029/2005JA011584, 2007.

Shen, C., Y. Y. Yang, Z. J. Rong, X. Li, M. Dunlop, C. M. Carr, Z. X. Liu, D. N. Baker, Z. Q. Chen, Y. Ji, G. Zeng: Direct calculation of the Ring Current distribution and magnetic structure seen by Cluster during Geomagnetic Storms, *J. Geophys. Res-Space Phys*, 119, doi:10.1002/2013JA019460, 2014.

Tsyganenko, N. A.: Modeling the Earth's magnetospheric magnetic field, confined within a realistic magnetopause, J. Geophys. Res., 100, 5599–5612, 1995.

Tsyganenko, N. A.: Effects of the solar wind conditions on the global magnetospheric configuration as deduced from data-based field models, in: Proceedings of the Third International Conference on Substorms (ICS-3), Versailles, France, 12–17 May 1996, edited by: Rolfe, E. and Kaldeich, B., Eur. Space Agency Spec. Publ., ESA-SP, 389, 181–185, 1996.

Tsyganenko, N. A., H. J. Singer, and J. C. Kasper: Storm-time distortion of the inner magnetosphere: How severe can it get?, J. Geophys. Res., 108(A5), 1209, doi:10.1029/2002JA009808, 2003.

Vallat, C., I. Dandouras, M. Dunlop, A. Balogh, E. Lucek, G. K. Parks, M. Wilber, E. C. Roelof, G. Chanteur, and H. Rème: First current density measurements in the ring current region using simultaneous multispacecraft CLUSTER-FGM data, Ann. Geophys., 23,1849–1865, 2005.

Wang, H., Lühr, H., Ma, S. Y., Weygand, J., Skoug, R. M., and Yin, F.: Field-aligned currents observed by CHAMP during the intense 2003 geomagnetic storm events: Ann. Geophys., 24, 311-324, 2006.

Yang, Y. Y., C. Shen, M. Dunlop, Z. J. Rong, X. Li, V. Angelopoulos, Z. Q. Chen, G. Q. Yan, and Y. Ji: Storm time current distribution in the inner equatorial magnetosphere: THEMIS observations, J. Geophys. Res. Space Physics, 121, doi:10.1002/ 2015JA022145, 2016.

Zhang, Q.-H., et al.: The distribution of the ring current: Cluster observations, Ann. Geophys., 29, 1655–1662, 2011.